

STATUS OF THE MAGIC-II MIRRORS

Markus Garzarczyk DESY

August 2013

Abstract

This document summarises the current status of the MAGIC-II mirrors. It includes the study of the mirror surface deformations, the improvement of the mirror surface reflectivity after cleaning of the mirrors as well as the results from mirror surface reflectivity measurements performed up to now. Finally all the measurements are combined and candidates of mirrors with bad quality are defined.



CONTENTS

1	Mirror surface quality	3
1.1	Measurement description	3
1.2	The MAGIC-II reflector	3
1.3	Surface deformation on the Al mirrors	4
1.4	Surface deformation on the glass mirrors	5
1.5	Summary	7
2	Mirror cleaning effect	8
2.1	Measurement description	8
2.2	Cleaning method	9
2.3	Results from the mirror surface reflectivity measurements	10
2.3.1	Averaged reflectivity distributions	10
2.3.2	Effect of dust deposit on the different mirror types	11
2.4	Summary	13
3	Mirror surface reflectivity	15
3.1	Measurement errors	15
3.2	Reflectivity measurements	16
3.3	Long term behaviour of the mirror surface reflectivity	18
4	Selection of mirrors for exchange	22
A	Images of the MAGIC-II reflector	24
B	Reflectivity measurements of MAGIC-II mirrors	41

1 MIRROR SURFACE QUALITY

1.1 Measurement description

Monitoring of the mirror surface quality at MAGIC started several years ago on the MAGIC-I telescope. The MAGIC-I mirrors showed a high grade of mirror surface deformations. The deformation of the $50 \times 50 \text{ cm}^2$ Al sandwich structure mirrors is an developing process, leading in worst case to detachment of the pre-milled and diamond polished Al front sheet plate.

The inspection itself was initially a visible check of the mirror surface, identifying the worst mirrors for exchange. An alternative method to quantify the grade of the deformation is nowadays performed by photographing the mirrors from near the focal distance. The trick is to focus the camera lens onto the mirror surface. By doing so the distant reflected objects become defocussed and mirror deformations become visible. As of now the analysis is performed manually, by inspecting the images and estimating the mirror surface percentage affected by the deformation.

For MAGIC-II the reflector was photographed in this way for the first time in January 2013. The procedure was repeated again in June 2013. No significant change in-between this two measurement periods was found. However, several mirrors with deformed mirror surface were identified. The results shown in this report are based on the most recent status, e.g. June 2013.

The image on the first page of this document shows an example of some MAGIC-II mirrors, as found in June 2013. The complete set of images, marked also with the corresponding mirror numbers, is included in the appendix A, at the end of this document.

1.2 The MAGIC-II reflector

Two different mirror types are installed on the MAGIC-II telescope. The central region is filled with 1 m^2 Al sandwich structure mirrors. These mirrors were produced using the same technique as for the small size MAGIC-I Al mirrors. The main difference of the design is the double size ($4\times$ larger surface) as well as the fact that the MAGIC-II mirrors do not have an integrated heating system. The outer region of the MAGIC-II reflector is filled with glass mirrors, produced with the so called cold slumping technique. Figure 1 illustrates the distribution of the different mirror types on the MAGIC-II telescope. In total 143 Al mirrors and 104 glass mirrors are installed on the MAGIC-II reflector. There are 6 glass mirrors, where one edge was cut in order to allow installing them at the following places:

- 4 such mirrors are installed close to the elevation axis, where the steel wires for the telescope camera bowl are fixed. These are the mirror numbers $(-8,1)$, $(-8,-1)$, $(8,1)$ and $(8,-1)$.
- 2 such mirrors are installed on the lower edges of the telescope reflector, where standard mirrors would collide with the telescope support structure. These are the mirror numbers $(-4,-8)$ and $(4,-8)$.

Due to their different design, the Al and glass mirrors will be handled separately in this report. Chapter 1.3 describes the status of the Al mirrors, while chapter 1.4 describes the status of the glass mirrors.

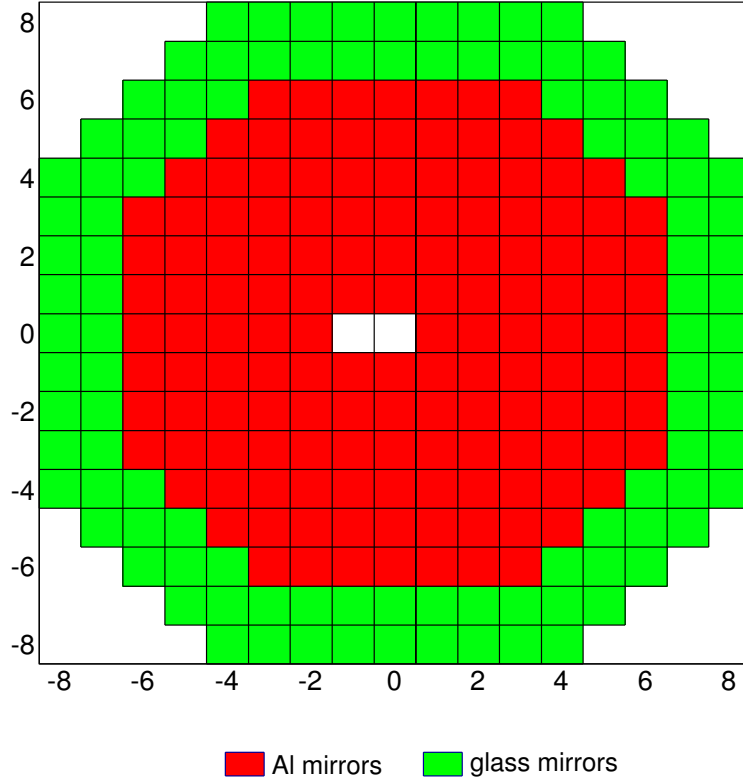


Figure 1: Distribution of the two different mirror types on the MAGIC-II telescope. The inner area (red) of the reflector is filled using 143 Al sandwich structure mirrors. The outer ring (green) of the reflector is filled with 104 glass mirrors made using the cold slumping technique.

1.3 Surface deformation on the Al mirrors

The front cover of this document shows an image of the Al mirrors on MAGIC-II. As seen on this picture as well as on the additional pictures in the appendix A of this report, the 1 m^2 Al mirrors show a significant effect of degradation of the mirror surface. Almost all mirrors have at least a small percentage of deformations. In most cases the deformations are along the sides of the mirror. There are 15 mirrors ($\sim 10.5\%$ of all Al mirrors), where the deformation reached an area $> 5\%$ of the total mirror area.

It has to be mentioned that the quality control of the MAGIC-II Al mirrors was significantly improved in comparison with MAGIC-I. All large 1 m^2 mirrors were immersed in a water bath before being shipped to the telescope site. Holes found during the immersion test (identified as place where air bubbles are created) were closed with UV resistant glue. This immersion test was performed in order to guarantee that mirror damages, as found on the small MAGIC-I mirrors, do not accrue in MAGIC-II.

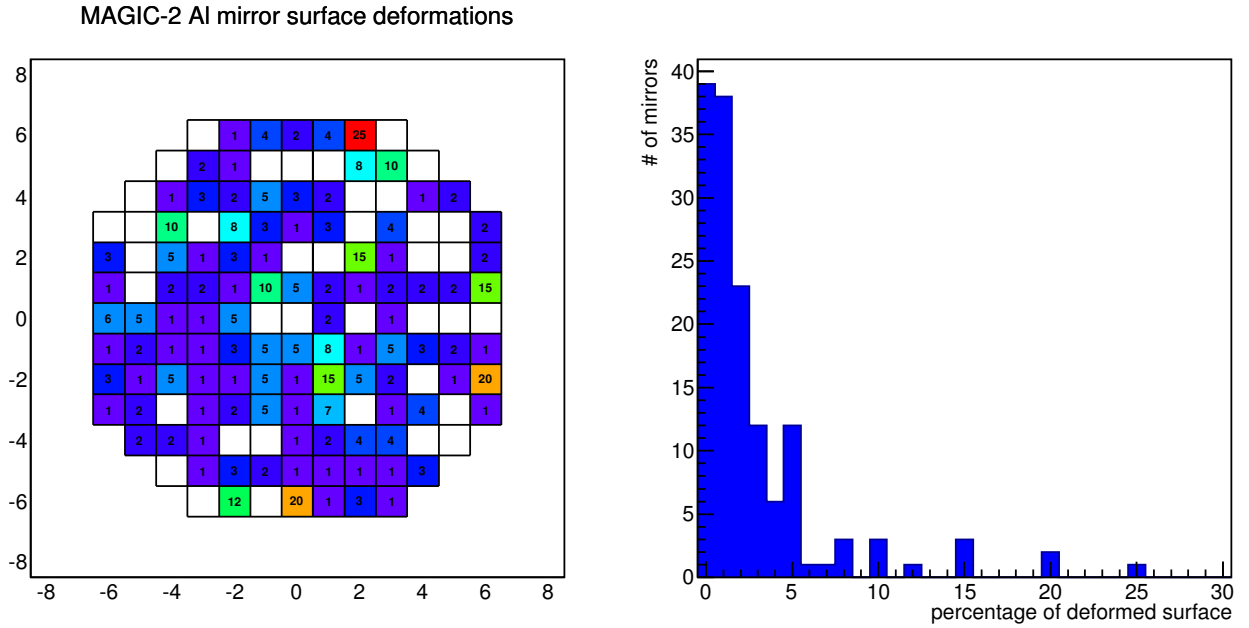


Figure 2: Mirror surface deformations of the 1 m² Al mirrors on the MAGIC-II telescope, as measured in June 2013. The numbers in the left plot correspond to the percentage of mirror surface affected by deformations. The right plot shows the distribution of the deformations.

1.4 Surface deformation on the glass mirrors

Glass mirrors are made with a different technology. In general one would not expect to see the same problems as on the Al mirrors.

For the Al mirrors the believed reason for the mirror surface deformation is based on the fact that there is water inside the mirror structure. Ultrasonic measurements of some mirrors affected by the deformations showed the presence of condensed water inside the honey comb cells. The condensed water expands when forming ice in the winter time and produces internal forces on the mirror walls. The weak point is the glue between the honey comb structure and the Al front plate. The glued surface detaches along the affected area filled with water and releases the internal stress of the machined Al front plate. This results in a local change of the the radius of curvature, which than becomes visible as bubbles.

The glass mirrors are made of a thin glass sheet, pressed at high temperature and with high pressure to the mould, which than gives the required radius of the mirror. The glass mirrors are made water tight with silicone and a protective plastic L profile along the sides. One would expect to see cracks along the glass sheet if strong internal forces generated during ice formation would be present. No cracks on the mirrors were found until now.

Figure 3 show the percentage of the mirror area of the glass mirrors affected by surface deformations. When comparing with Al mirrors, glass mirrors are showing less bubbles. In total 6 mirrors ($\sim 5.8\%$ of all glass mirrors) show deformations $> 5\%$. Two examples of bubbles on glass mirrors are shown in figure 4, more images are included in the appendix A.

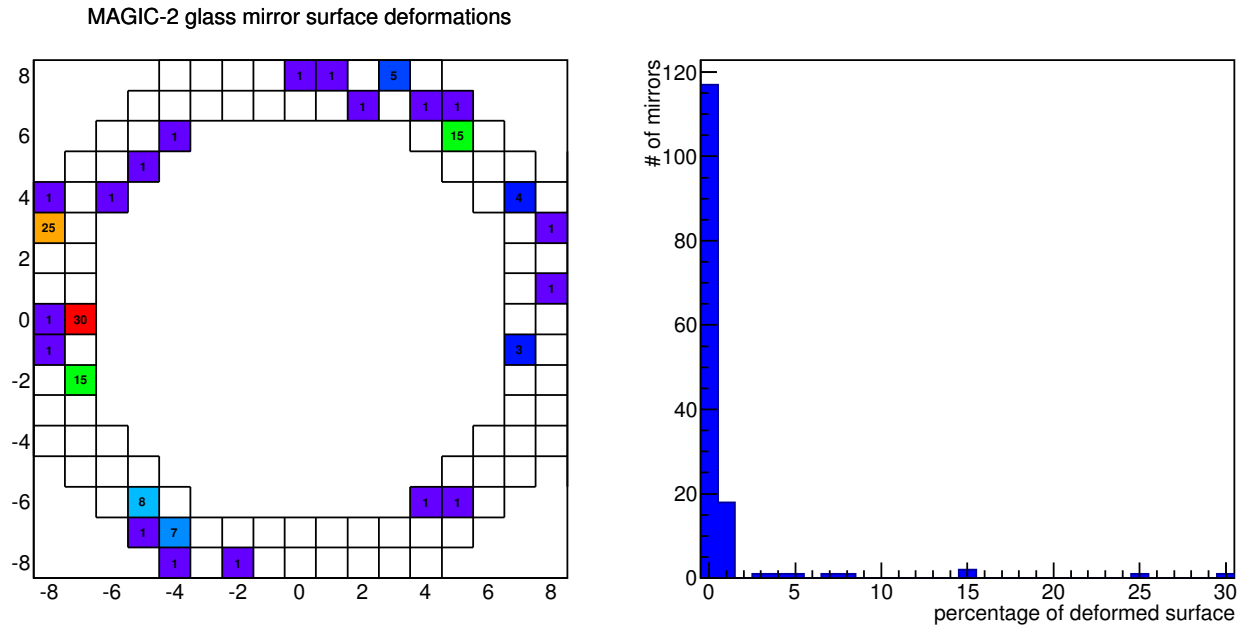


Figure 3: Mirror surface deformations of the 1 m² glass mirrors on the MAGIC-II telescope, as measured in June 2013. The numbers in the left plot correspond to the percentage of mirror surface affected by deformations. The right plot shows the distribution of the deformations.

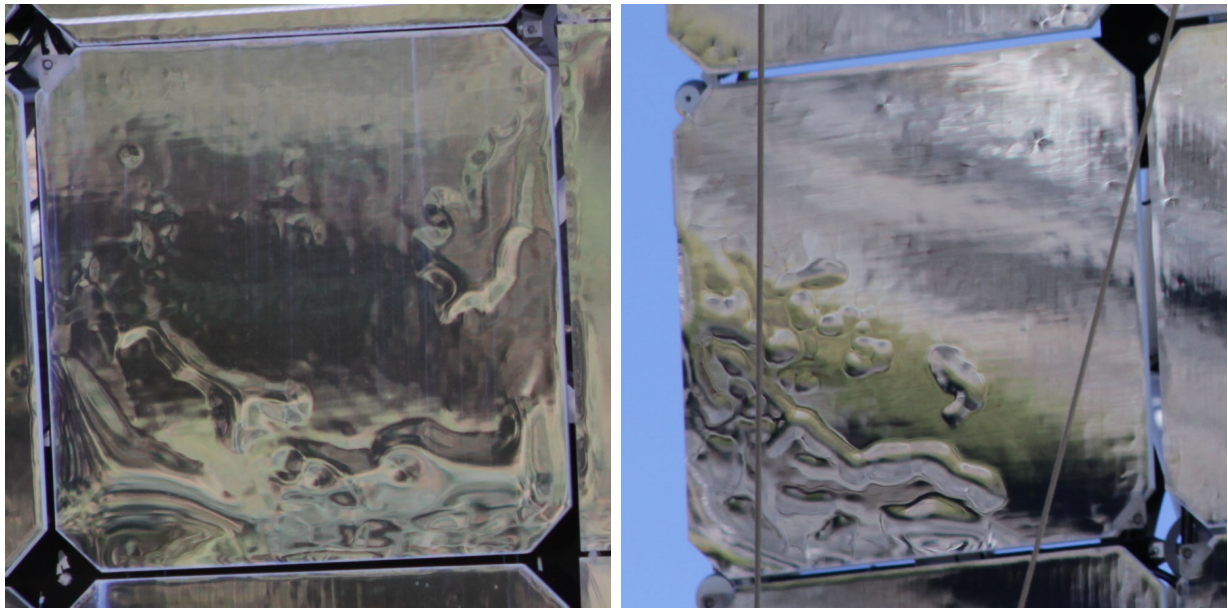


Figure 4: Two examples of glass mirrors showing the presence of mirror surface deformations. On the left the mirror (-7,0), on the right the mirror (-8,3). The mirror (-7,0) shows about 30% of deformed mirror surface. The mirror (-8,3) shows 25%.

1.5 Summary

Figure 5 shows once more the complete view of the MAGIC-II reflector, indicating the percentage of the mirror area affected by bubbles. There are in total 21 mirror segments with deformations $> 5\%$. The sum of all the mirror deformations result in a total area of 2.12%. This corresponds to a mirror surface of 5.23 m². This mirror area is generating an diffuse PSF component and should therefore be removed from the effective mirror area used in Monte Carlo simulations. There are 133 mirrors affected by bubbles (54% of all mirrors installed on the telescope). Most of the Al mirrors show deformations on the edges of the mirrors, which partially result from the production process (milling of the Al plate).

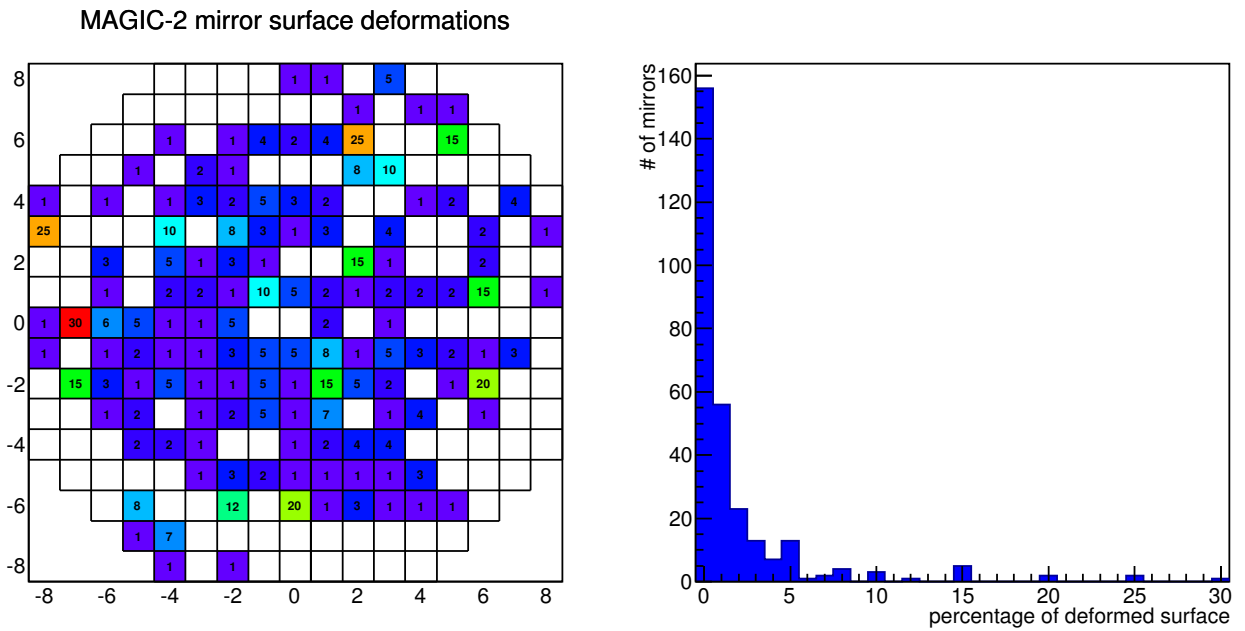


Figure 5: Mirror surface deformations of the complete MAGIC-II reflector. The numbers in the left plot correspond to the percentage of mirror surface affected by deformations. The right plot shows the distribution of the deformations.

2 MIRROR CLEANING EFFECT

2.1 Measurement description

The reflectivity measurement was performed using the IRIS 908RS device borrowed from the TNG telescope (see figure 6). The device is operating at four different wavelengths. The four laser diodes have the following characteristics:

- **B:** $\lambda = 470 \text{ nm}$ (FWHM = 30 nm)
- **G:** $\lambda = 530 \text{ nm}$ (FWHM = 40 nm)
- **R:** $\lambda = 650 \text{ nm}$ (FWHM = 30 nm)
- **IR:** $\lambda = 880 \text{ nm}$ (FWHM = 80 nm)

The laser diodes focus their beam of light at an inclination angle of 45° in respect to the sample surface. Four detectors are mounted at 0° , $+2^\circ$, -15° and -45° . The later three are used to determine the scattering component of the reflected light. For the analysis presented in this report only the reflected component at 0° (emitted light beam angle same as the reflected light beam angle) is used. Following the device data sheet, the maximal relative error of the instrument and therefore the measurement accuracy is 0.5%. The repetitiveness of the reflectivity measurement was measured at a MAGIC mirror. 30 consecutive measurements were performed at the same place. The repetitiveness was measured to be $\pm 0.20\%$ for B, $\pm 0.23\%$ for G, $\pm 0.18\%$ for R and $\pm 0.33\%$ for IR wavelengths. These values are higher than the value of 0.1% for 20 measurements given in the device data sheet. The measured area is 10 mm in diameter. Chapter 3.1 summarises the systematic errors of this measurement.

Each mirror was measured at eight points: four at the corners of the mirror and four in the central area of the mirror (see figure 7). The same measurement procedure was followed for all the mirrors.



Figure 6: IRIS 908RS2 reflectometer

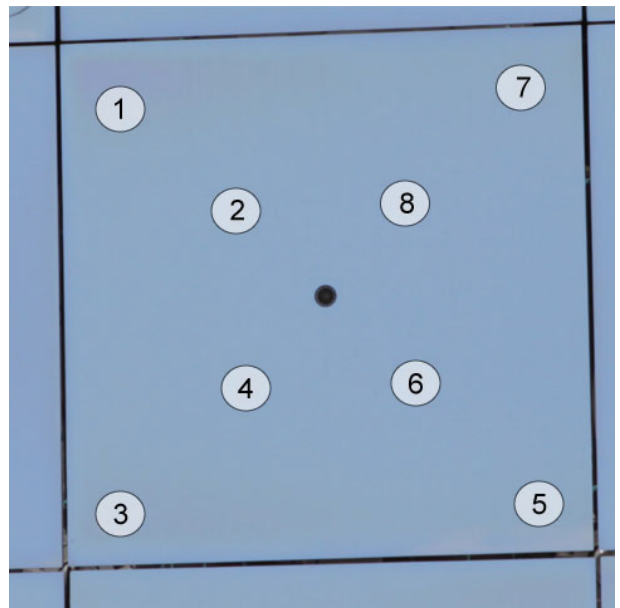


Figure 7: Places on the mirror and the order how the reflectivity measurement was performed.

2.2 Cleaning method

Visual inspection of the mirrors at MAGIC-II have shown that there is a significant dust deposit on the mirror surface during the summer time. The MAGIC mirrors are not cleaned manually. The mirror surface is cleaned only by rain, e.g. mainly in the winter period (December - April). This means that the dust deposit will increase slowly during the summer time, resulting in a degrading reflectivity.

In order to verify the effect of the dust deposit on the mirror surface reflectivity, several mirrors were cleaned by hand. The cleaning was done with clean water and a soft tissue, making sure that the protective surface of the mirror is not damaged or scratched.

The test was performed on July 27th, 2013. The following mirrors were cleaned: (0,-1), (1,-1), (2,-1), (0,-2), (1,-2), (2,-2), (7,-2), (8,-2), (0,-3), (1,-3), (2,-3), (5,-3), (6,-3), (7,-3), (8,-3), (3,-4), (4,-4), (5,-4), (6,-4), (7,-4), (8,-4), (3,-5), (4,-5), (6,-5), (7,-5), (2,-6), (3,-6), (4,-6), (2,-7), (3,-7) and (4,-7).

The image below show the effect of the mirror cleaning. The mirror in the left upper corner shows dirty surface, while the other mirrors, especially the one on the right lower corner was cleaned and do not show so strong dust deposit anymore.

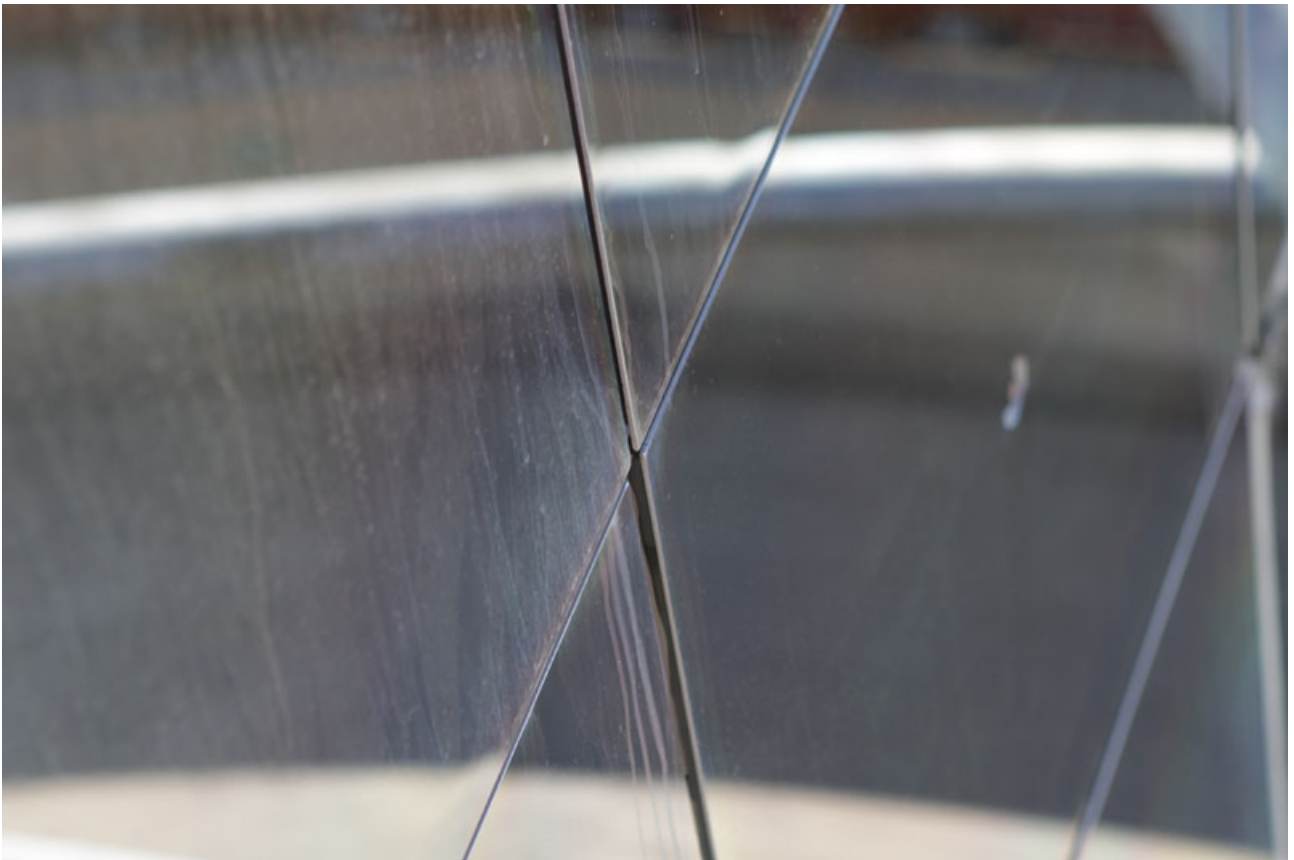


Figure 8: Image showing a dirty mirror surface (left upper mirror) and a cleaned surface (right lower mirror).

2.3 Results from the mirror surface reflectivity measurements

2.3.1 Averaged reflectivity distributions

Figure 9 shows the distribution of the measured reflectivity values of mirrors before (filled histogram) and after cleaning (shadowed histogram). The four different distributions are for the different wavelengths provided by the reflectometer. At all four wavelengths one can see an enhancement of the mirror surface reflectivity after the cleaning of the mirror surface.

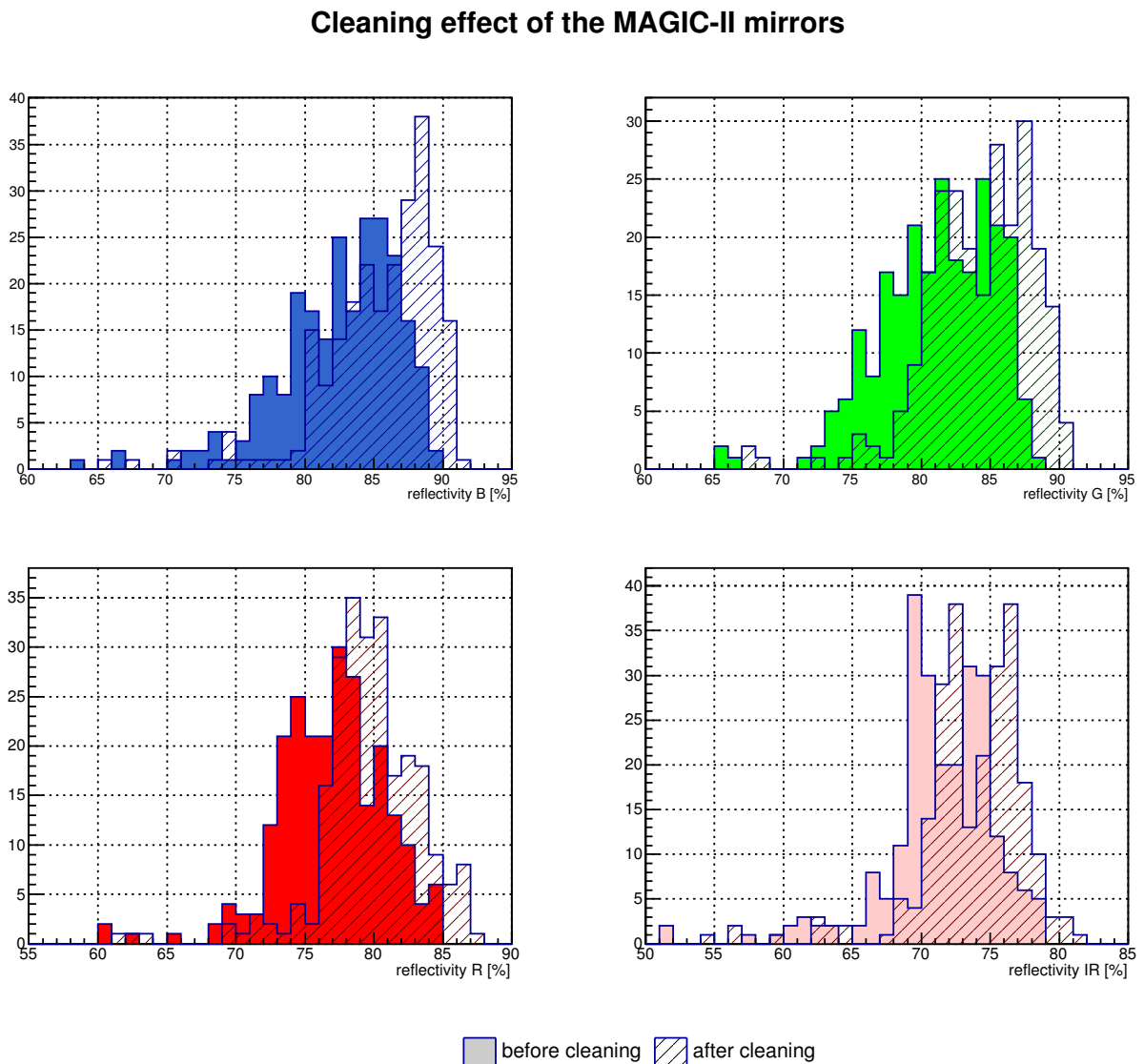


Figure 9: Distribution of the mirror reflectivity for the wavelengths measured before cleaning (filled histograms) and after the cleaning (shadowed histograms).

Figure 10 show the numerically calculated mean values of this distributions before and after cleaning. The reflectivity error bars include the standard deviations of the distributions as well

as the repetitiveness errors. The mean surface reflectivity enhancement after the cleaning is the range between 2.3% and 3.1%, dependent on the wavelength range.

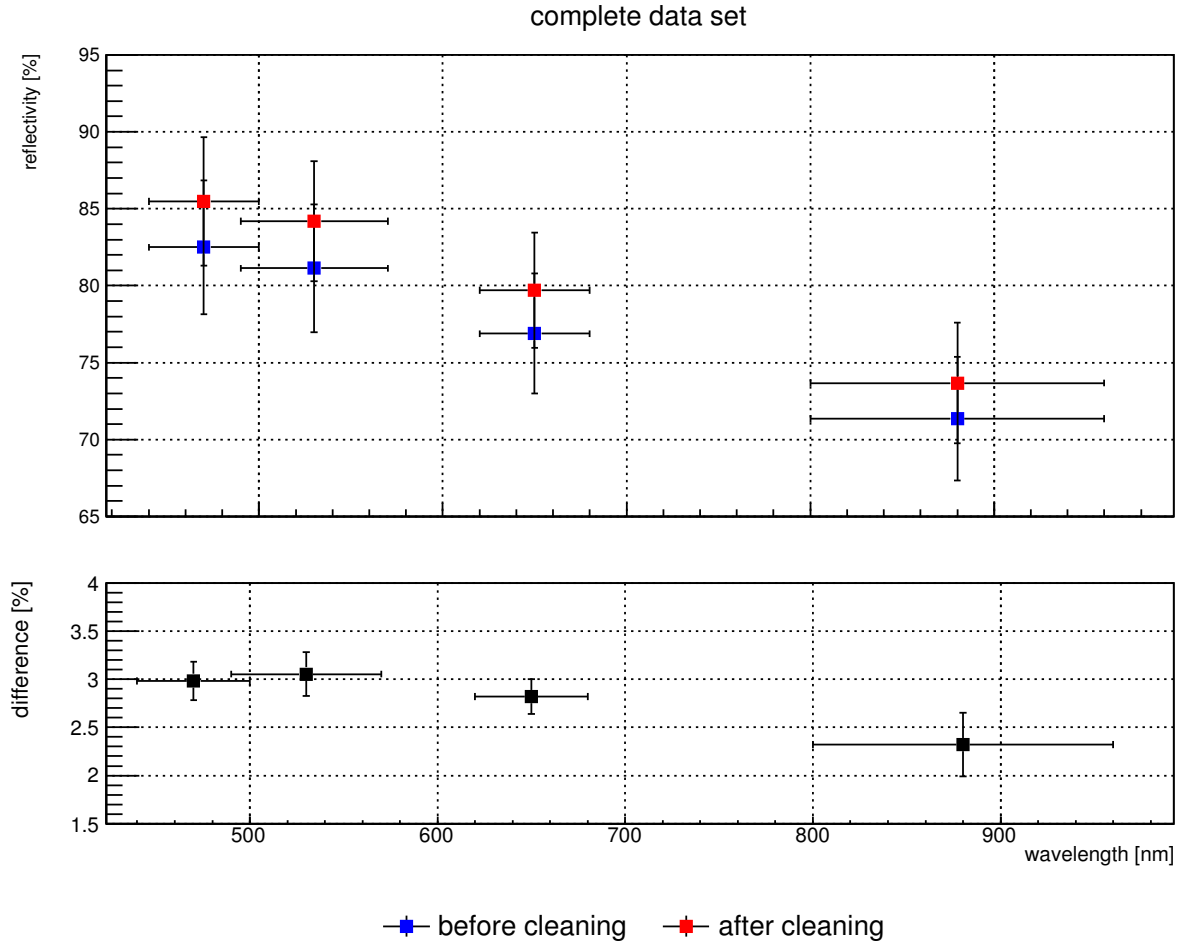


Figure 10: Averaged reflectivity before and after mirror cleaning. The lower plot shows the shift of the mean value for the different wavelengths after the mirror cleaning.

The results shown above do not separate the different mirror types (glass / aluminium). The separation will be discussed in the next part of this document.

2.3.2 Effect of dust deposit on the different mirror types

In the following the results are split to separate the aluminium and glass mirrors. The first analysis concentrates on the blue wavelength range at 470 nm, as this is the most interesting region for IACTs.

Figure 11 show the enhancement of the mirror surface reflectivity after mirror cleaning for the glass mirrors (upper row) and the aluminium mirrors (lower row). The figure on the left shows all measured data points, while the figure on the right shows the difference between the dirty and cleaned mirror. This number is an average of the 8 individual measurement points per mirror. An positive number means an enhancement of the mirror surface reflectivity after the

cleaning. From the gauss fit to the distribution one can see an enhancement of 2.31% for the glass mirrors and 3.41% for the aluminium mirrors. The value is rounded due to the selected bin width of the histogram. The more accurate number comes from the numerical calculation, shown in figure 12.

Cleaning effect of the MAGIC-II mirrors

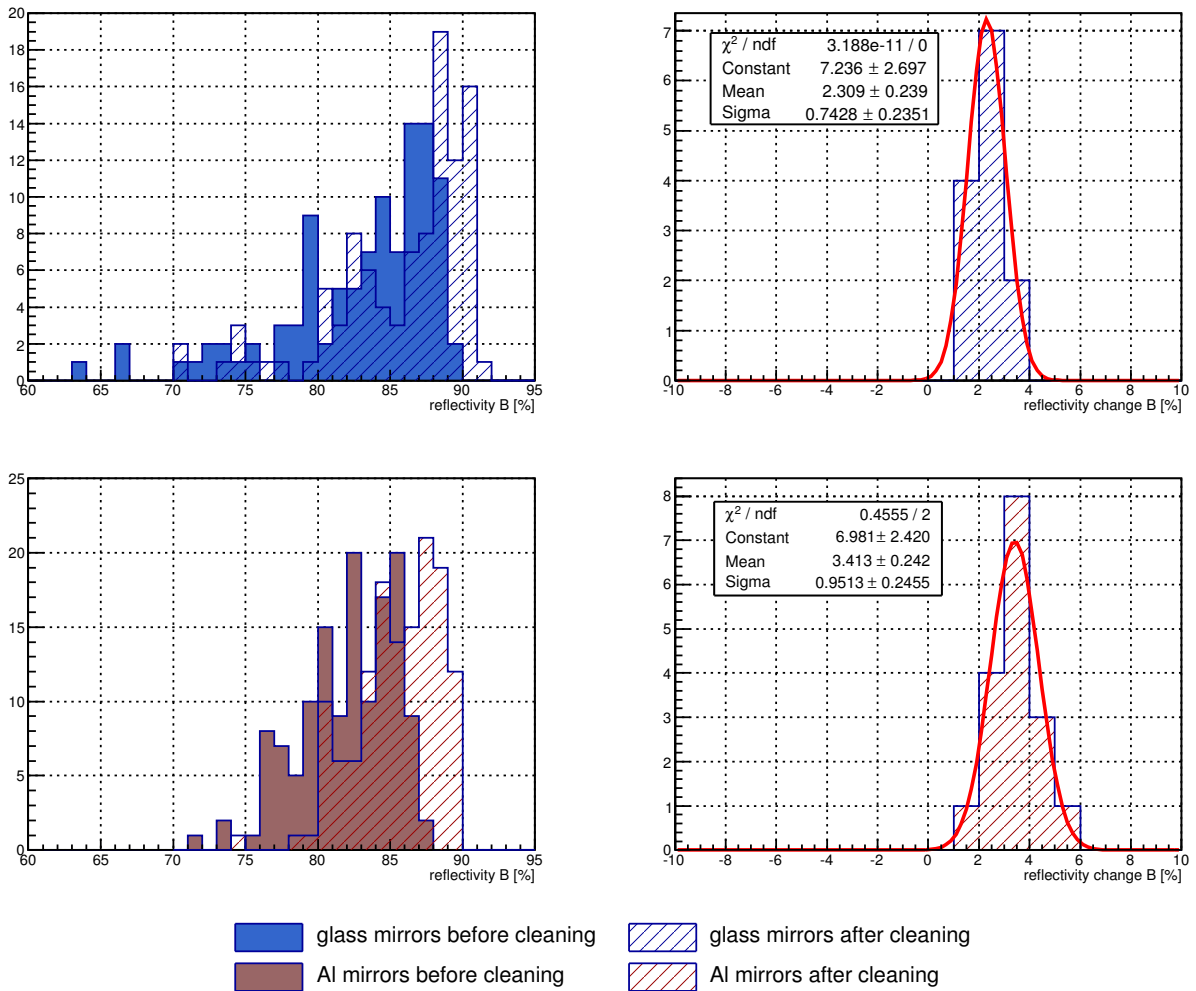


Figure 11: Distribution of the mirror reflectivity at 470 nm for the different mirror types. The upper row represents the glass mirrors, the lower row represents the aluminium mirrors. The histograms on the left show all the measurements for the particular mirror type before (filled area) and after the cleaning (shaded area). The histograms on the right side show the change of the mirror surface reflectivity after cleaning, averaged over the 8 measurements for each individual mirror.

Figure 12 shows the change of the reflectivity for glass and aluminium mirrors at the different wavelengths after the mirror cleaning. An enhancement of the mean reflectivity is present at all wavelengths for both mirror types. The enhancement is significantly higher for the aluminium

mirrors. The reason is due to the higher surface roughness, when compared with the glass mirrors. The maximum effect is pronounced for both mirror types at 530 nm.

Using this numbers and taking into account the percentage of aluminium and glass mirrors installed, one can estimate an collective loss of reflectivity for the MAGIC-II reflector to be 2.99% at 470 nm and 3.07% at 530 nm. These numbers are more accurate than the average of only measured mirrors as was shown in chapter 2.3.1.

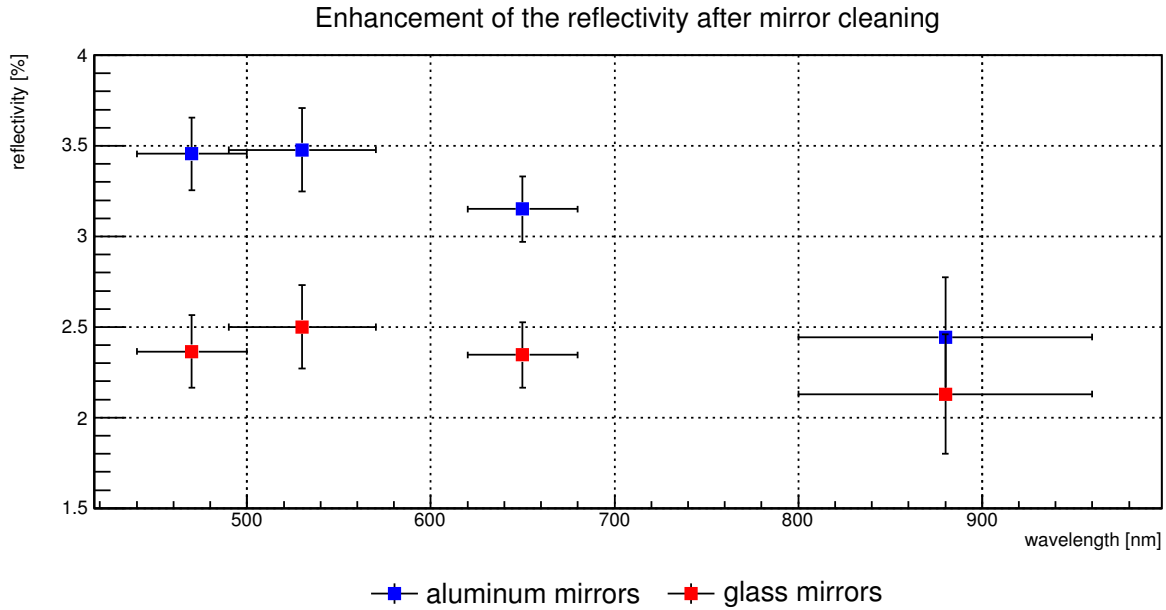


Figure 12: Mean enhancement of the mirror surface reflectivity for the aluminium and glass mirrors after mirror cleaning.

2.4 Summary

The effect of reflectivity loss due to dust deposit on the MAGIC-II mirrors was studied already back in April 2011. At this time only 8 aluminium mirrors were cleaned and measured in the same way as described in this document. At this time the dust deposit was not strong. Glass mirrors were found to be clean. From the measurement in 2011 the gain of surface reflectivity after cleaning was between 1.2% and 1.7%, dependent on the wavelength range. At 470 nm the change was 1.53%.

The status of the mirrors in June 2013 showed stronger dust deposit. Even glass mirrors were found to have a dust layer. The reason could be a larger time period since the last rain season (difference between April and June) or a close by Calima event. Measurement from June 2013 showed an reflectivity loss of 3.45% at 470 nm for the aluminium mirrors and 2.37% for the glass mirrors. The difference between this two values is due to the higher surface roughness of the diamond milled aluminium mirrors. The dust sticks stronger to a more rough surface.

An averaged loss in reflectivity by 2.99% can be translated to a reduced mirror area of about 7 m². It has to be mentioned, that the values obtained using this method are only an lower limit.

The mirror surface reflectivity does not properly characterise the performance of IACT mirrors, other than in optical telescopes, where the mirror quality is significantly better. The best parameter to characterise the mirror performance is the focussed reflectivity. This parameter is significantly lower than the mirror surface reflectivity as it includes also large scale mirror surface deformations, which cannot be measured using a hand-held reflectometer. It is therefore expected that the dust deposit has a larger effect on the reduced reflectivity than obtained from this analysis.

Remark: One might improve the telescope performance by regularly cleaning the mirrors in MAGIC-I and MAGIC-II. At VERITAS cleaning of the mirrors is an regular maintenance step (called 'optical wash'), performed at each full Moon period. The procedure was described by Emmet Roache (roache@veritas.sao.arizona.edu) in the following way:

"Basically what we do is a large scale version of what is often called an "optical wash", this means we wash from bottom to top to bottom. We use a pressure washer with a soap reservoir. The soap we use is called "Liqui-Nox" made by a company called Alconox (Factory address: 61 Cornelison Ave., Jersey City, NJ 07304 U.S.A.). We use this soap because it is biodegradable, phosphate free and completely soluble in water (i.e. it leaves no trace residue after rinsing). The soap is concentrated so we only use about 10 ml per liter of water. We have anodized aluminum mirrors which are more durable than bare aluminum. Using a pressure washer on bare aluminum would likely lead to aluminum loss.

For washing a telescope I start by rinsing with water only, from the bottom, working in quadrants. For example I will rinse the lower left quadrant and then apply soap to that quadrant. Then rinse the lower right with water and then apply soap to the lower right. Then rinse the upper left with water and apply soap. Rinse the upper right, then apply soap in the upper right. After I have worked from the bottom up it is time to rinse from the top down. Rinse the upper right and the upper left, then moving down to rinse the lower right and lower left. There is some over lap between quadrants to make sure all mirrors are cleaned. Each individual mirror facet is also cleaned from bottom to top to bottom. If there is a bit of wind or very dirty mirrors I will split the scope into six sections instead of just four. I wash the telescopes every month during the full moon. I continue to wash the telescope during the summer shutdown even though we are not observing because any bird droppings left on the mirrors will degrade the coating if not cleaned off relatively quickly.

Since Oct. 2011 we now do the final rinse with distilled water. Our local water is "hard" and we found it was leaving mineral deposits behind, especially during the summer months (evaporation is very quick around here).

Overall, the effects on reflectivity improvement depends on how dirty the mirrors are. During the springtime we have a lot of wind and dust, so washing can improve the reflectivity by 5 to 8% (at most). For the majority of the year 1 to 5% would be a typical improvement. We should have more data on the effects of washing on reflectivity later on this year when the collaboration further improves its ability to quickly measure whole dish reflectivity."

The enhancement of the mirror reflectivity after the optical wash at the VERITAS telescopes is compatible with the numbers obtained at MAGIC.

3 MIRROR SURFACE REFLECTIVITY

Regular mirror surface reflectivity measurements of the MAGIC-II reflector started in August 2009 and were repeated since then in regular time intervals. The measurements were performed always with the same IRIS 908RS reflectometer borrowed from the TNG telescope. Details about the measurement procedure can be found in chapter 2.1. It is easier now to compare the different results obtained over the time span of several years, by using data from the same reflectometer device.

3.1 Measurement errors

The following systematic errors have been investigated and taken into account during the analysis:

1. Measurement accuracy of the IRIS 908RS reflectometer.

The number for the accuracy of the measurement was taken from the data sheet of the instrument. The manufacturer quotes an accuracy of 0.5% for all four wavelength bands. There might be an time dependent degradation of the absolute number obtained with the reflectometer. The calibration of the device is done regularly with a reflectivity standard sample. However, no information about the stability of the calibration gauge exists. It is not known when the reference mirror of the gauge was certified the last time. The analysis shown here assumes a stable calibration of the device and an accuracy of $\pm 0.5\%$.

The error on the measurement accuracy is applied only when absolute reflectivity numbers are provided. For the computation of the relative reflectivity changes this contribution can be ignored.

2. Measurement repetitiveness of the IRIS 908RS reflectometer.

The measurement repetitiveness was measured on one MAGIC-II mirror. 30 consecutive measurements were performed at the same place of the mirror, without displacement of the reflectometer head. The repetitiveness of the measurement was determined using the maximum spread of the measured values around the mean. Table 1 shows the results for the different wavelengths. The values for the different wavelengths quoted in the last column will be used. It has to be mentioned, that the repetitiveness quoted in the data sheet is with 0.1% much smaller than in reality.

wavelength	mean [%]	upper edge [%]	lower edge [%]	repetitiveness [%]
470 nm	87.49	0.11	-0.09	0.20
530 nm	86.42	0.12	-0.11	0.23
650 nm	81.12	0.10	-0.08	0.18
880 nm	73.47	0.17	-0.16	0.33

Table 1: Repetitiveness of the IRIS 908RS reflectometer measured on a MAGIC-II mirror.

The repetitiveness of the measurement is a real systematic error and should be included in every analysis method discussed in this document.

3. Mean and standard deviation of the measured distribution.

The mean and standard deviation of the measured values is calculated numerically. A gaussian fit did not always converge and the numerical calculation seems to be more reliable, especially because it is not dependent on the binning size used to produce the histograms. The mean reflectivity is calculated using the following formula:

$$\mu = \frac{1}{N} \cdot \sum_{i=1}^N X_i \quad (1)$$

The variance of the distribution, e.g. square root of the standard deviation σ is calculated following the formula:

$$\sigma^2 = \frac{1}{N} \cdot \sum_{i=1}^N X_i^2 - \mu^2 \quad (2)$$

4. Cleanness of the mirrors.

Section 2 of this document describes the reflectivity loss due to dust deposit on the mirror surface. The mirror surface was not always measured at the same environmental conditions. The mirrors were not treated especially (e.g. cleaned) before the measurement was done. It turns out that the uncertainty about the cleanness of the mirrors generates the largest uncertainty for the understanding of the reflectivity degradation.

The reflectivity loss due to dust deposit is wavelength and mirror type dependent. The increase of the reflectivity after mirror cleaning is shown in figure 12. The uncertainty of the measured reflectivity value at any time in the year due to dust can be as high as 3.5% (at 470 nm) for aluminium mirrors and 2.5% for the glass mirrors. These numbers can be even higher, as it is not guaranteed that the cleaning test performed in June 2013 was at the moment of worst dust deposit.

Due to their large contribution, it makes no sense to include these numbers to the error budget of the degradation studies. However, the limits (figure 12) will be displayed as shadowed area in some plots.

3.2 Reflectivity measurements

Figure 13 shows an example of the reflectivity values for the different mirrors of the MAGIC-II telescope. The values shown are extracted from the data taken in May 2013 for the 470 nm wavelength band. The figure on the right shows the difference between the aluminium and glass mirrors. In general, the aluminium mirrors have about 3% lower mean reflectivity than the glass mirrors. The distributions of the glass mirrors show larger standard deviation. The reason is a significant amount of glass mirrors with reflectivity $\ll \mu$. Figures for the other wavelengths as well as previous measurement periods are included in the appendix B on page 41.

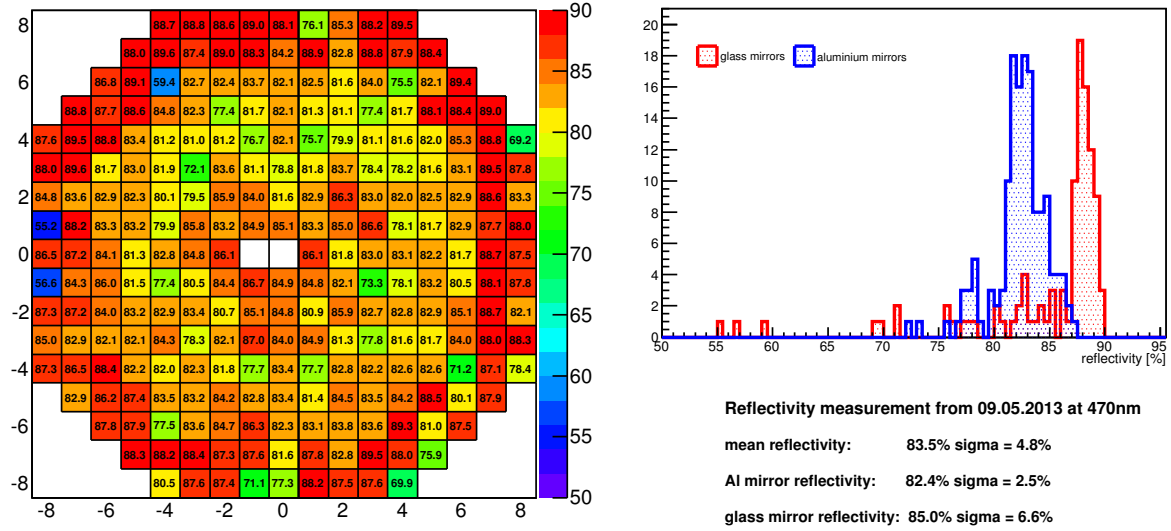


Figure 13: Mirror surface reflectivity at 470 nm.

The table 2 summarises the mean reflectivity of MAGIC-II and their individual contribution from aluminium and glass mirrors for the different time intervals. It is difficult to compare the results for the different measurement periods shown in this table. On the one hand, only the two data sets from April 2011 and May 2013 include nearly all mirrors mounted on the MAGIC-II telescope. In the other cases only a fraction of the telescope reflector was measured. On the other hand, the reflectivity change due to dust deposit is in the same range as the fluctuations of the mean reflectivity within the different data sets.

λ	mirror type	3.08.2009	20.10.2009	8.04.2011	9.05.2013	27.07.2013
470 nm	all	$84.2 \pm 2.7\%$	$84.8 \pm 2.6\%$	$85.5 \pm 3.4\%$	$83.5 \pm 4.8\%$	$82.5 \pm 4.1\%$
	glass	$86.5 \pm 1.6\%$	$86.2 \pm 3.1\%$	$86.6 \pm 4.6\%$	$85.0 \pm 6.6\%$	$83.0 \pm 5.4\%$
	aluminium	$82.9 \pm 2.3\%$	$83.8 \pm 1.4\%$	$84.7 \pm 1.7\%$	$82.4 \pm 2.5\%$	$82.0 \pm 1.4\%$
530 nm	all	$83.2 \pm 1.7\%$	$83.4 \pm 2.2\%$	$83.9 \pm 2.9\%$	$82.3 \pm 4.1\%$	$81.2 \pm 3.6\%$
	glass	$84.3 \pm 1.1\%$	$84.5 \pm 1.8\%$	$84.9 \pm 3.5\%$	$84.2 \pm 5.1\%$	$81.7 \pm 4.5\%$
	aluminium	$82.6 \pm 1.7\%$	$82.6 \pm 1.8\%$	$83.2 \pm 2.0\%$	$81.0 \pm 2.4\%$	$80.6 \pm 1.9\%$
650 nm	all	$79.0 \pm 1.7\%$	$79.0 \pm 1.9\%$	$79.2 \pm 2.4\%$	$77.9 \pm 3.2\%$	$76.8 \pm 3.1\%$
	glass	$79.6 \pm 0.6\%$	$79.7 \pm 1.6\%$	$79.7 \pm 3.0\%$	$79.0 \pm 4.4\%$	$76.8 \pm 3.9\%$
	aluminium	$78.8 \pm 2.0\%$	$78.6 \pm 1.9\%$	$78.8 \pm 1.8\%$	$77.1 \pm 1.4\%$	$76.7 \pm 1.8\%$
880 nm	all	$72.7 \pm 2.9\%$	$73.5 \pm 2.2\%$	$74.0 \pm 2.6\%$	$72.9 \pm 3.8\%$	$71.4 \pm 3.4\%$
	glass	$76.1 \pm 1.7\%$	$75.5 \pm 1.9\%$	$75.4 \pm 3.2\%$	$73.2 \pm 5.5\%$	$71.9 \pm 4.4\%$
	aluminium	$70.8 \pm 1.3\%$	$72.1 \pm 1.1\%$	$73.1 \pm 1.2\%$	$72.7 \pm 1.7\%$	$70.9 \pm 1.3\%$

Table 2: Mean reflectivity values measured during the different time intervals. The errors represent the standard deviation of the distributions.

3.3 Long term behaviour of the mirror surface reflectivity

In order to quantify a possible degradation of the mirror surface reflectivity over time and reduce the effect of possible up/down scatter of the values due to unknown surface cleanness one can compute the difference of the reflectivity in respect to a clean mirror.

In June 2013 a large fraction of aluminium and glass mirrors was cleaned and remeasured (see section 2.2). Mirrors contained in this data set (data set B) are used as reference. To compute the change of reflectivity versus previous measurements (data set A) only mirrors contained in both data sets (A and B) are used. The mirrors are treated individually, e.g. the mean reflectivity of a single mirror contained in A and B is subtracted from each other. The average as well as standard deviation of this values is than computed. The repetitiveness errors are included to the systematic error shown in the figures.

Remark: One is expecting a positive number from the difference A-B, as it would mean a loss of the reflectivity vs. time.

There are four aluminium mirrors, which were cleaned and measured in April 2011 as well as in June 2013. Using this data one can compute a representative limit on the reflectivity loss for aluminium mirrors for a time period of 27 months. Figure 14 shows this result for the different wavelength bands. From this small data set one can observe a marginal loss of reflectivity with an maximum of $\sim 1\%$ during the 27 months.

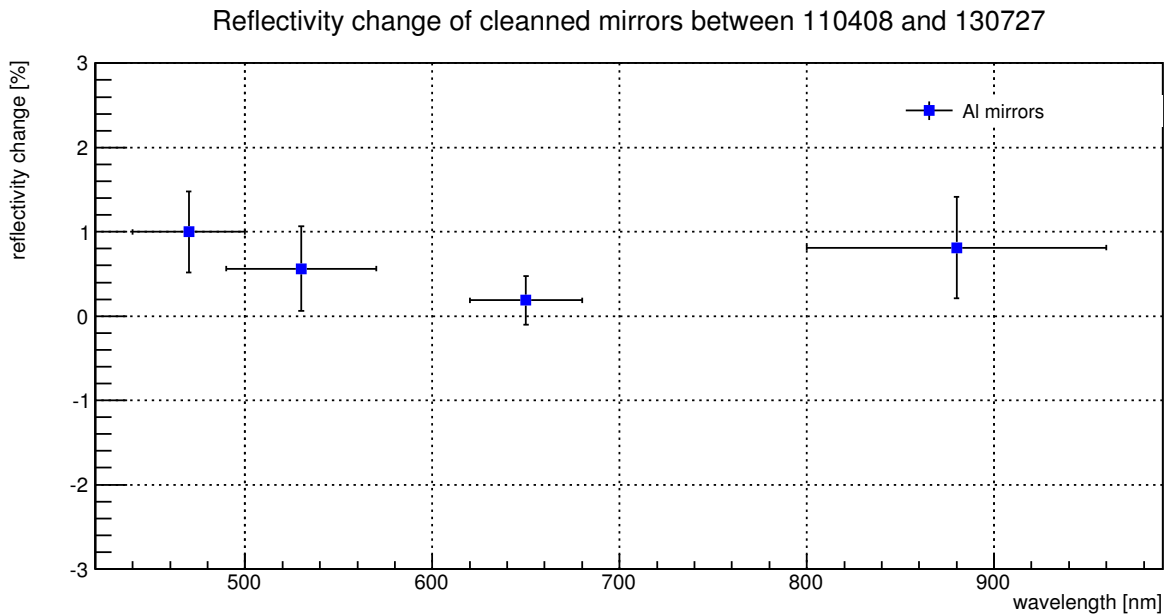


Figure 14: Change of the mirror surface reflectivity of cleaned MAGIC-II Al mirrors over a time period of 27 months. The results are the average of four 1 m^2 mirrors. The systematic error on reflectivity includes the standard deviation of the distributions as well as the repetitiveness error.

There is no equivalent data set for the glass mirrors. To compute a possible reflectivity loss for the glass mirrors as well as to see the trend over a larger time period, the other measurements can be used. However, this comparison is strongly affected by the cleanness of the mirror. Therefore also the error range resulting from the dust deposit is shown as shadowed area. The analysis is performed in the same way as done for the clean aluminium mirrors. The reflectivity change is now shown vs. time [MJD]. Figures 15, 16, 17 and 18 show the results for the different wavelength bands. The x-axis grid lines separate the different years. The first two data points are from the year 2009. There is one point in 2011 and two more points in 2013.

Figure 15 shows the change of reflectivity for the aluminium and glass mirrors at the wavelength band of 470 nm. The error for the cleanness of the mirror is shown only in the negative range as the resulting values are the difference in respect to a clean mirror, e.g. the mirrors could only be more dirty in the past, not cleaner as the reference from June 2013. Positive number means that the reflectivity was higher at the moment of the measurement. The consequence is that the positive number is a lower limit for the loss of reflectivity. Negative value means that the mirror reflectivity was worse in the past. It is unphysical to expect that the mirror surface reflectivity increases vs. time, the only explanation is dust deposit on the mirror during the measurement in the past.

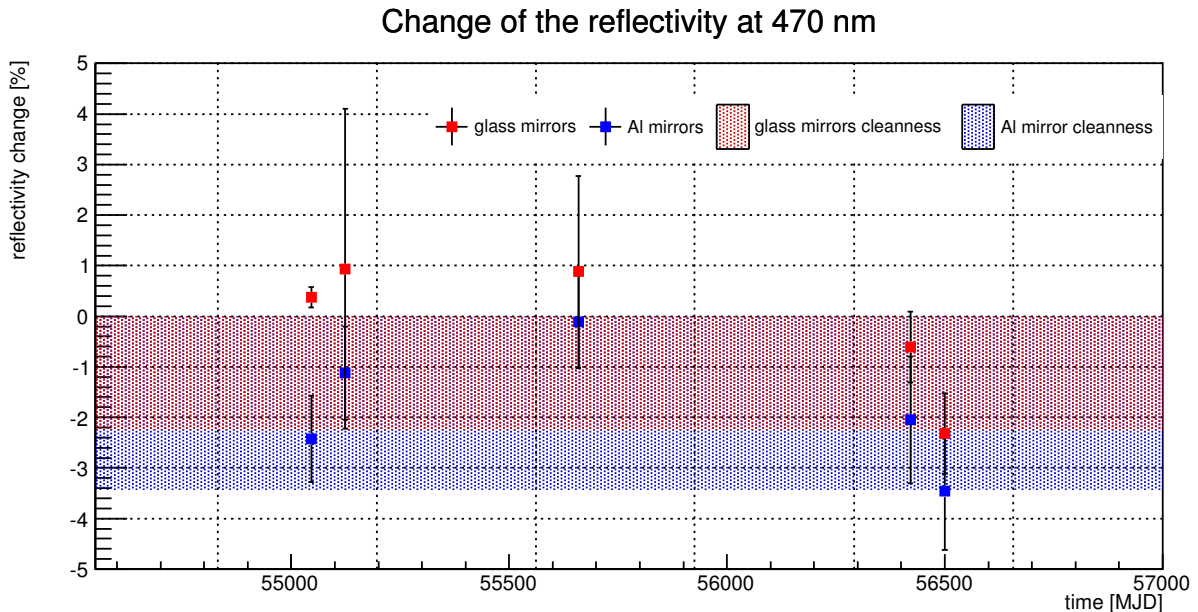


Figure 15: Long term stability of the mirror surface reflectivity at 470 nm.

The interpretation of the results shown in figure 15 is as follows:

- **Aluminium mirrors:** The difference of the reflectivity in respect to a clean mirror measured in June 2013 is in all cases negative. The reflectivity of a clean mirror now is higher than of the same mirror measured in 2009 and 2011. This means that the degradation is smaller than the error introduced by the dust deposit. The measurement performed in 2011 is close to the value obtained now. It indicates that the mirrors were

significantly cleaner than in 2009 and 2013. The cleanness of the aluminium mirrors in 2011 was investigated. The result was that the enhancement of the reflectivity after cleaning was 1.53% (see page 13). This number is compatible within error with the results obtained by comparison of the clean mirrors in 2011 and 2013.

- **Glass mirrors:** In 2009 and 2011 the values are positive, with a mean of $\sim 1\%$. This is the lower limit on the reflectivity loss from 2009 until 2013. One has to mention that the spread of the values is very large, indicated by the large error bars. There are mirrors with reflectivity loss of more than 4 % within this time period.
- In both cases the reflectivity measured in 2013 is negative, indicating that the measurement was performed during a time, where there was a strong dust deposit on both type of mirrors. The dust deposit was stronger in June 2013 than in May 2013.

Figures 16, 17 and 18 show the corresponding results for the wavelengths of 530 nm, 650 nm and 880 nm. The results are similar with the conclusions made above.

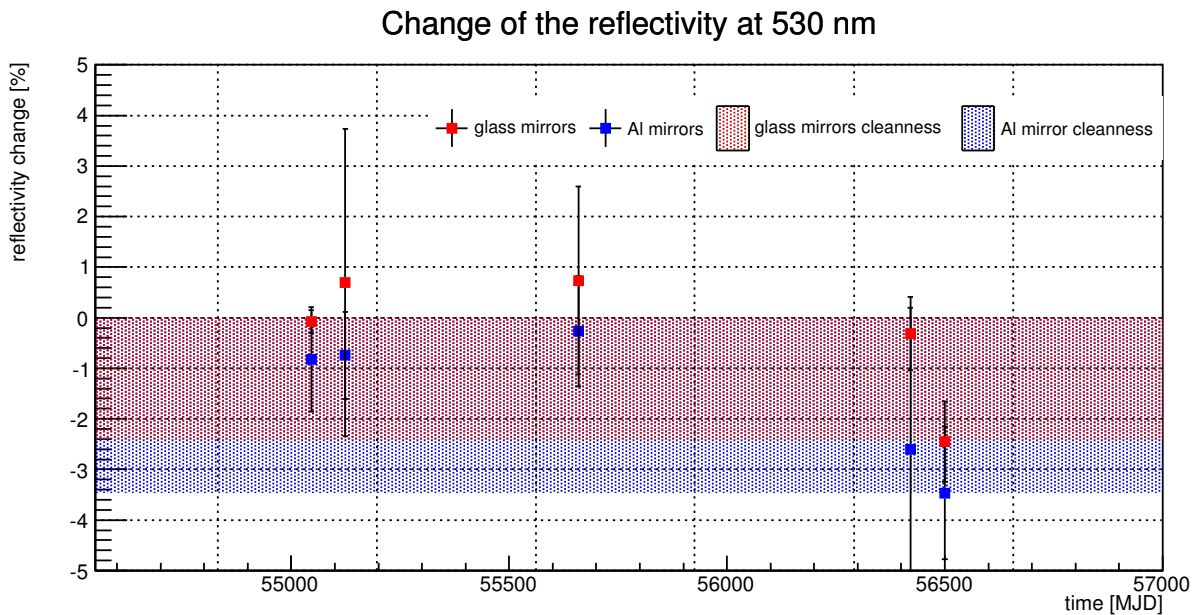


Figure 16: Long term stability of the mirror surface reflectivity at 530 nm.

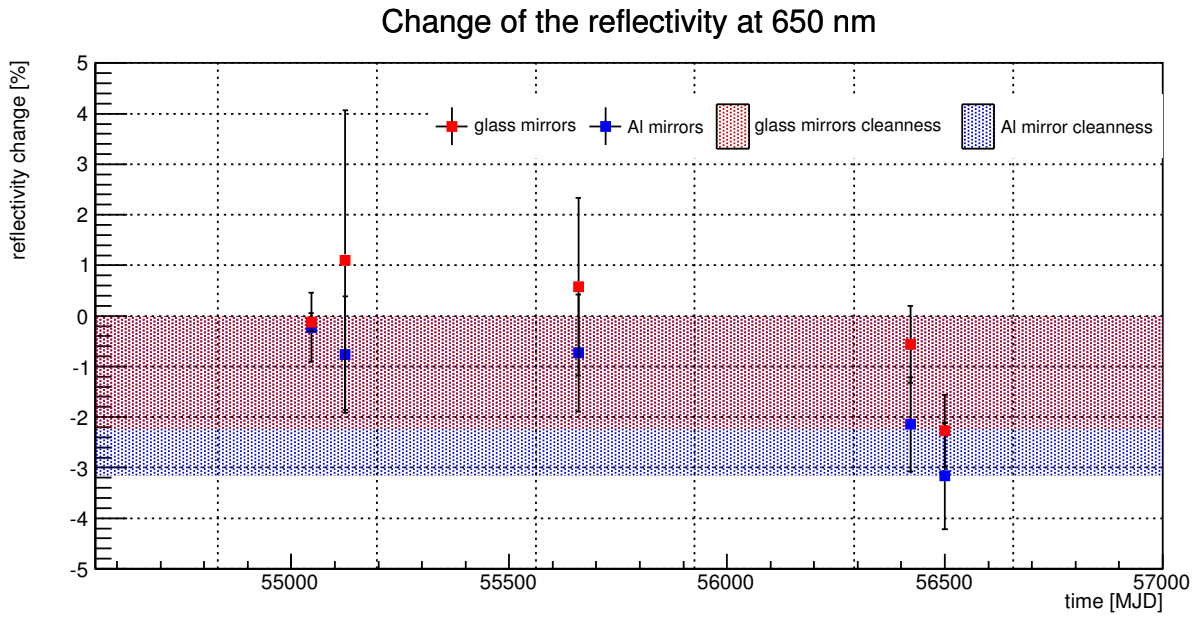


Figure 17: Long term stability of the mirror surface reflectivity at 650 nm.

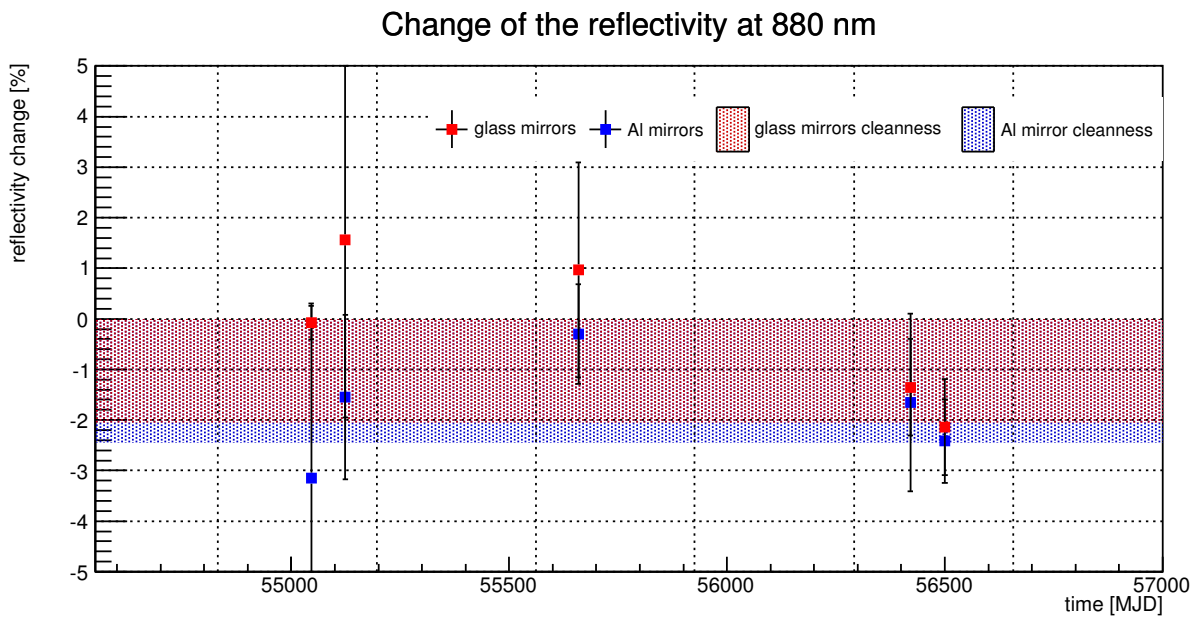


Figure 18: Long term stability of the mirror surface reflectivity at 880 nm.

4 SELECTION OF MIRRORS FOR EXCHANGE

In order to define the quality of an mirror the surface reflectivity is folded with the surface deformations, e.g. figure 13 with 5. The resulting values are shown in the figure 19. The distribution of the values is shown on the right hand side. In order to define a limit for a bad mirror, the mean μ as well as standard deviation σ of the distribution is computed. The $\mu - 3 \cdot \sigma$ defines the limit and is shown as red line in the histogram.

Using this approach not all mirrors with strong deformation were selected. Therefore a second limit of surface deformation $> 15\%$ was applied. The final selection of mirrors for exchange is shown in figure 20.

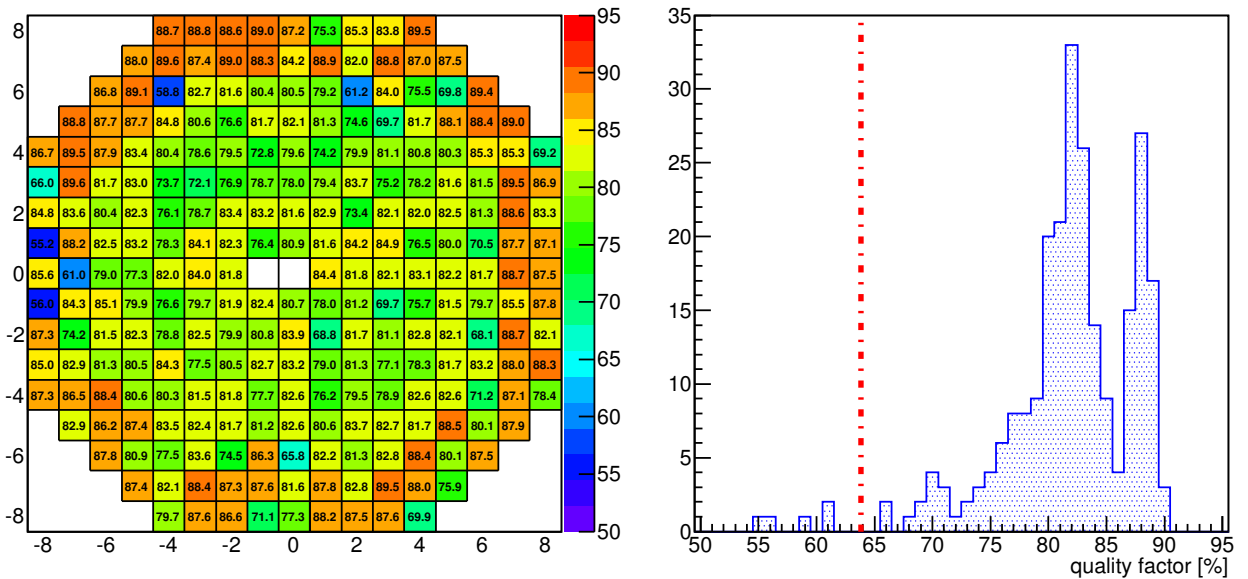


Figure 19: Quality of the MAGIC-II mirrors. Results are based on a folded surface reflectivity with the mirror surface deformations. The histogram on the right hand side shows the distribution of the values. The red line indicates the selected limit for mirrors to be exchanged.

There are $13 \times 1 \text{ m}^2$ mirrors, which were selected to be exchanged. 7 of them are glass mirrors and the rest are aluminium mirrors, mainly affected by surface deformations. Two of the glass mirrors are mounted close to the elevation axis $(-8,1)$ and $(-8,-1)$. These two mirrors are special, as they need an cut edge in order not to collide with the wires holding the camera bowl. The focal length of these mirrors is shown with different colour in the right histogram of figure 20. Table 3 summarises the characteristics of the mirrors, which were selected for exchange. Images of the mirrors can be seen in the appendix A.

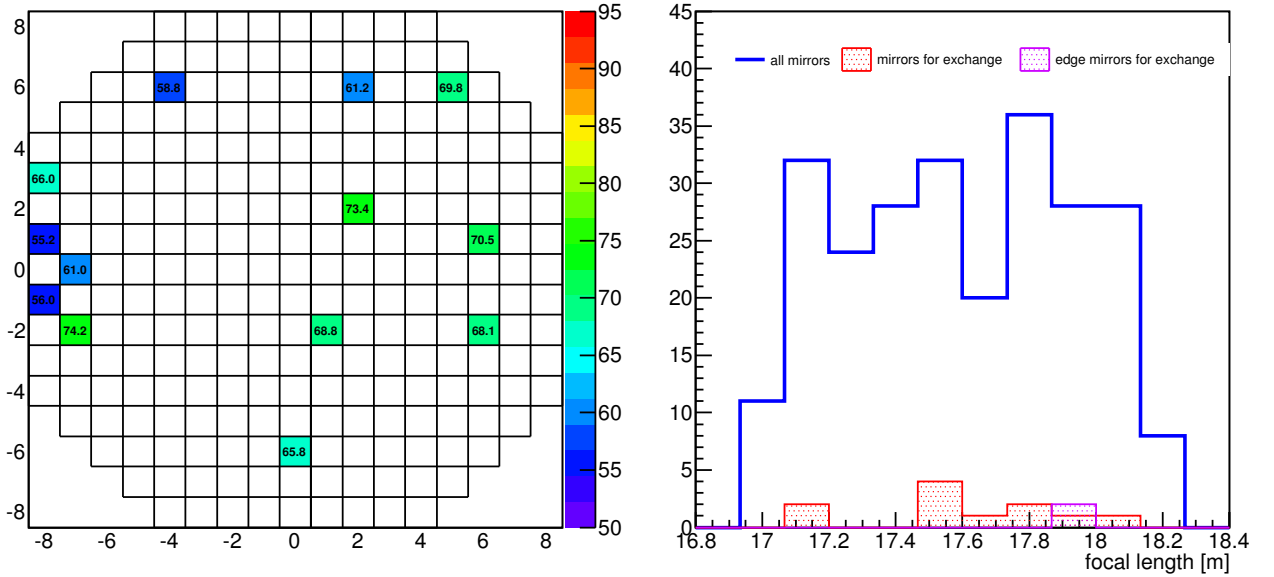
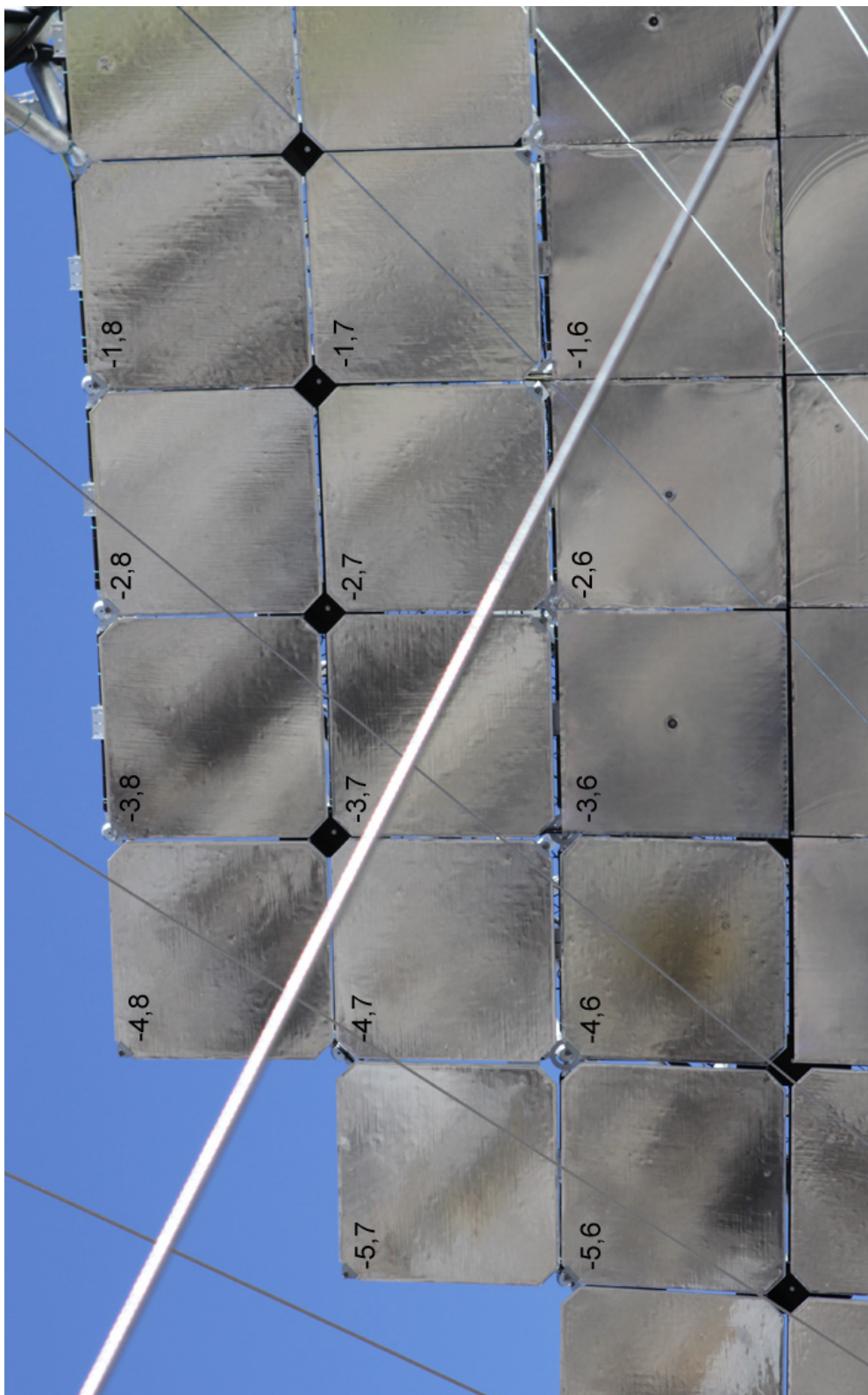


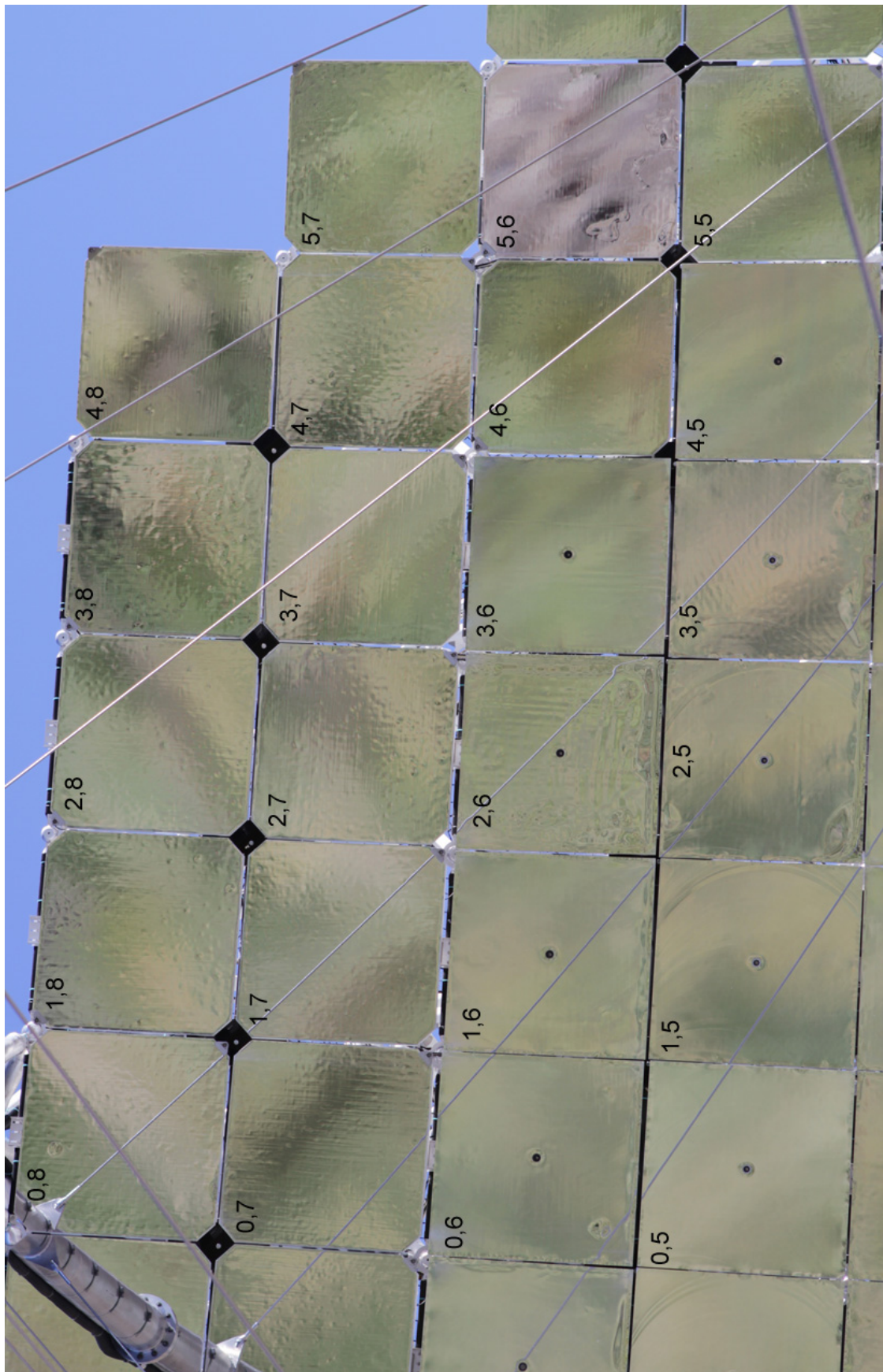
Figure 20: Mirrors selected for exchange. The focal length of the selected mirrors is shown on the right hand side.

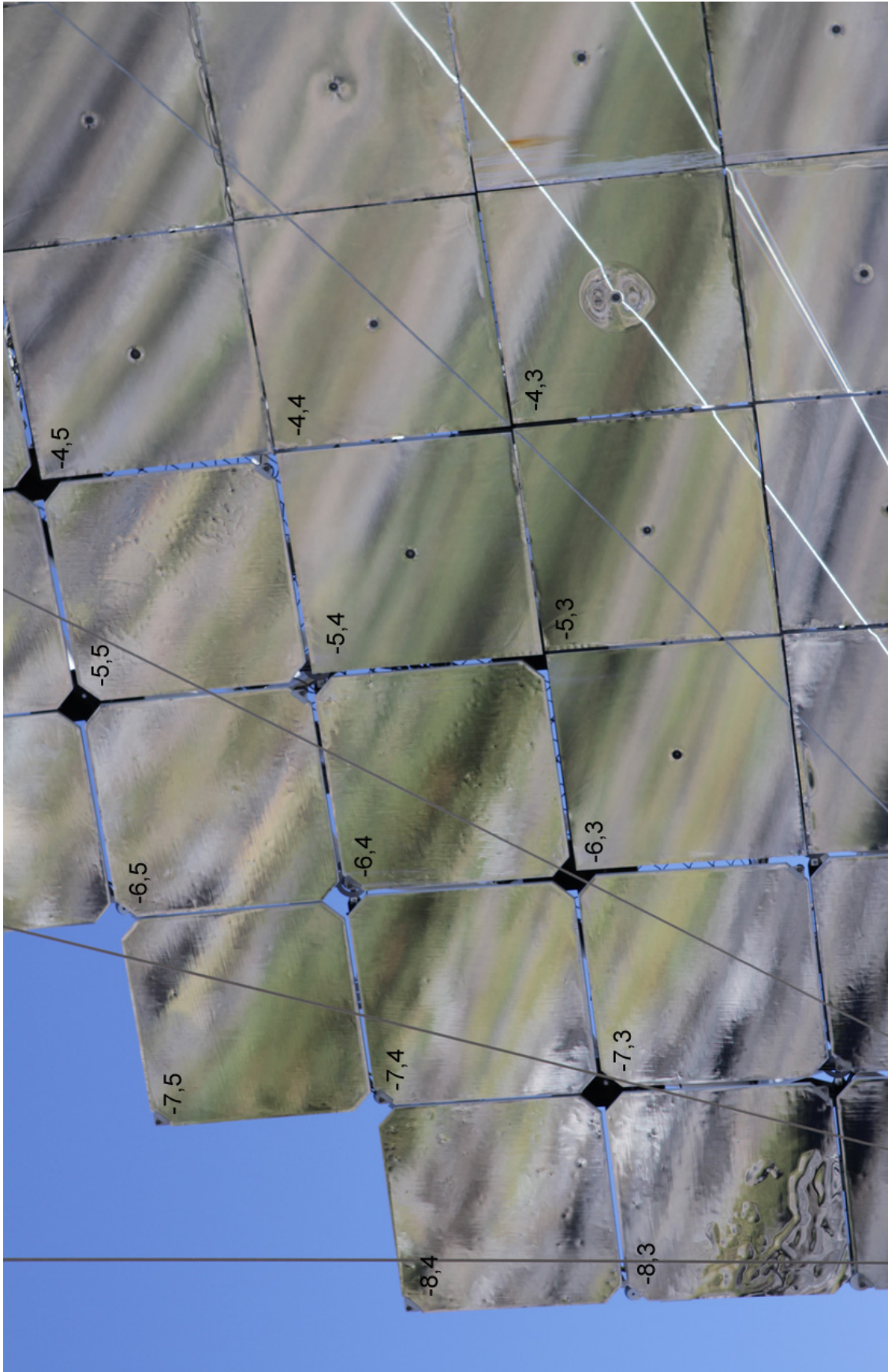
pos.	type	#	r [m]	nom. r [m]	ref. [%]	bubbles [%]	comb. [%]
(-8,-1)	glass/edge	T04	35.600	35.870	56.6	1	56.0
(-8,1)	glass/edge	T05	35.500	35.870	55.2	0	55.2
(-8,3)	glass	45	36.200	36.108	88.0	25	66.0
(-7,-2)	glass	21	35.600	35.511	87.2	15	74.2
(-7,0)	glass	18	35.421	35.391	87.2	30	61.0
(-4,6)	glass	97	35.421	35.481	59.4	0	58.8
(5,6)	glass	6	35.700	35.749	75.5	15	69.8
(0,-6)	Al	10	34.988	35.010	82.3	20	65.8
(1,-2)	Al	6	34.090	34.210	80.9	15	68.8
(2,2)	Al	9	34.230	34.180	86.3	15	74.3
(2,6)	Al	2	35.050	35.120	81.6	25	61.2
(6,-2)	Al	9	35.073	35.124	85.1	20	68.1
(6,1)	Al	5	35.019	35.035	82.9	15	70.5

Table 3: List of mirrors selected for exchange. Columns from left: position on the telescope, mirror type, mirror manufacturer number, radius of the mirror, nominal radius of the mirror, reflectivity as measured on 09.05.2013, percentage of deformed mirror surface, combined mirror quality.

A IMAGES OF THE MAGIC-II REFLECTOR

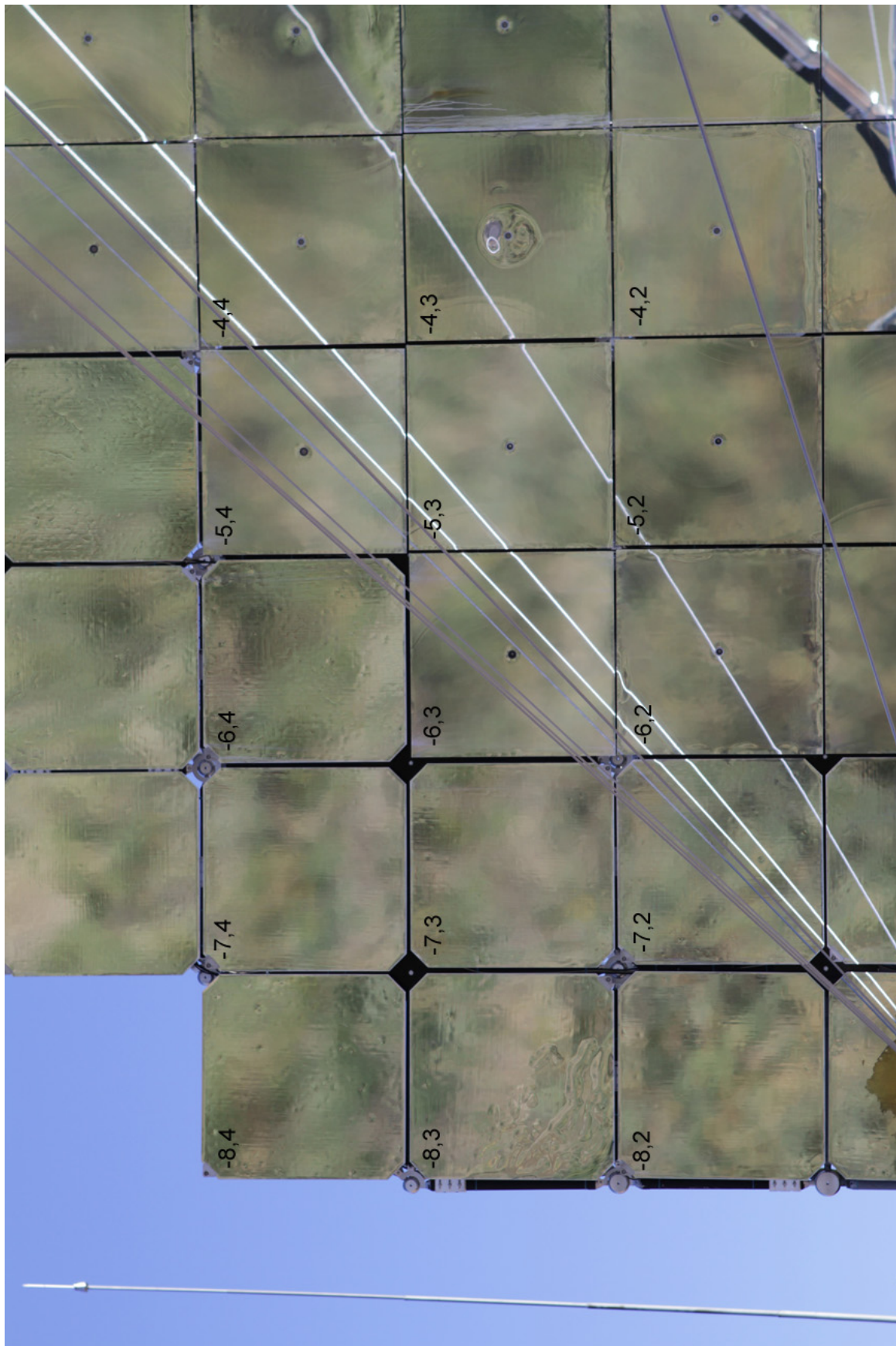




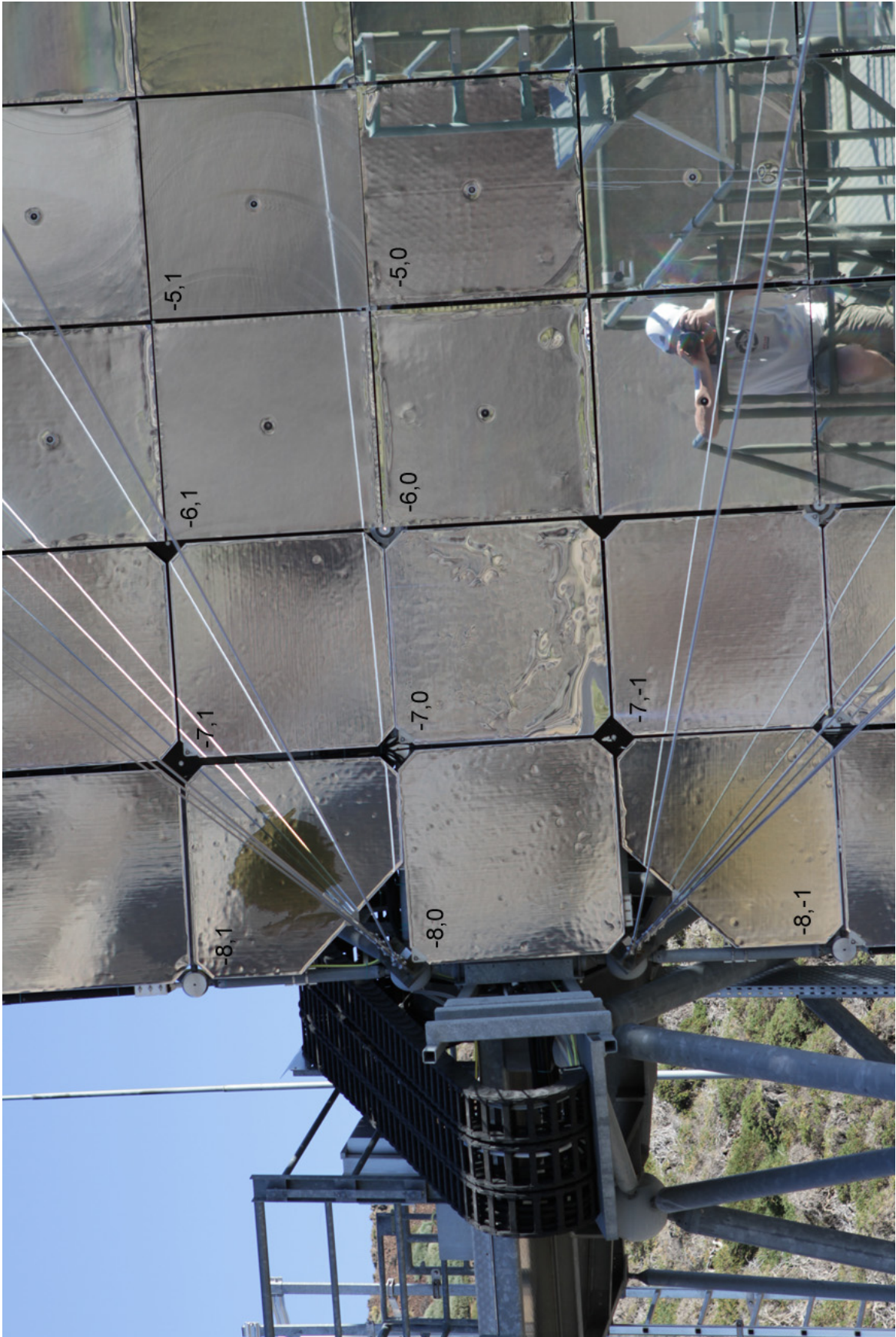










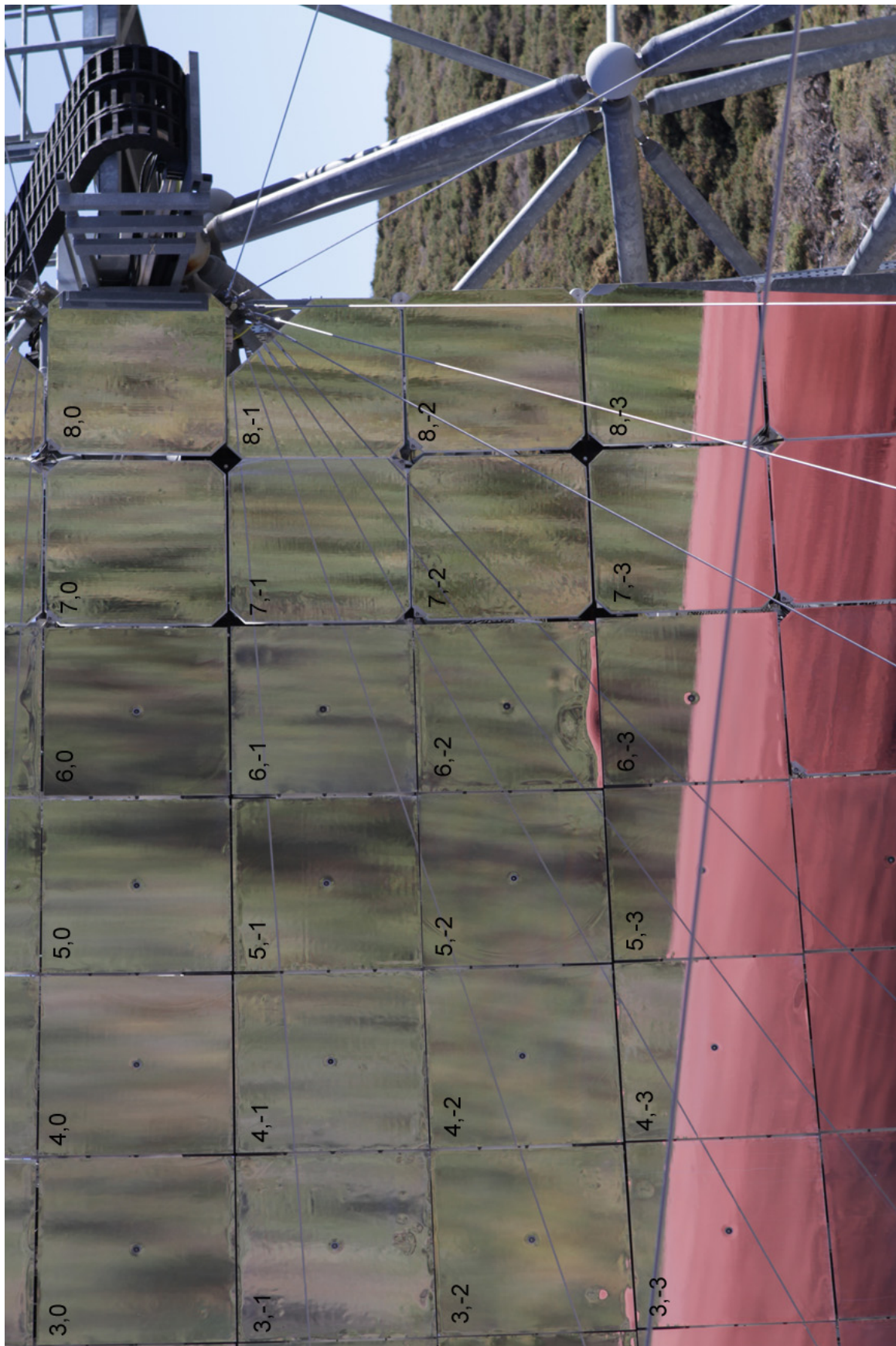






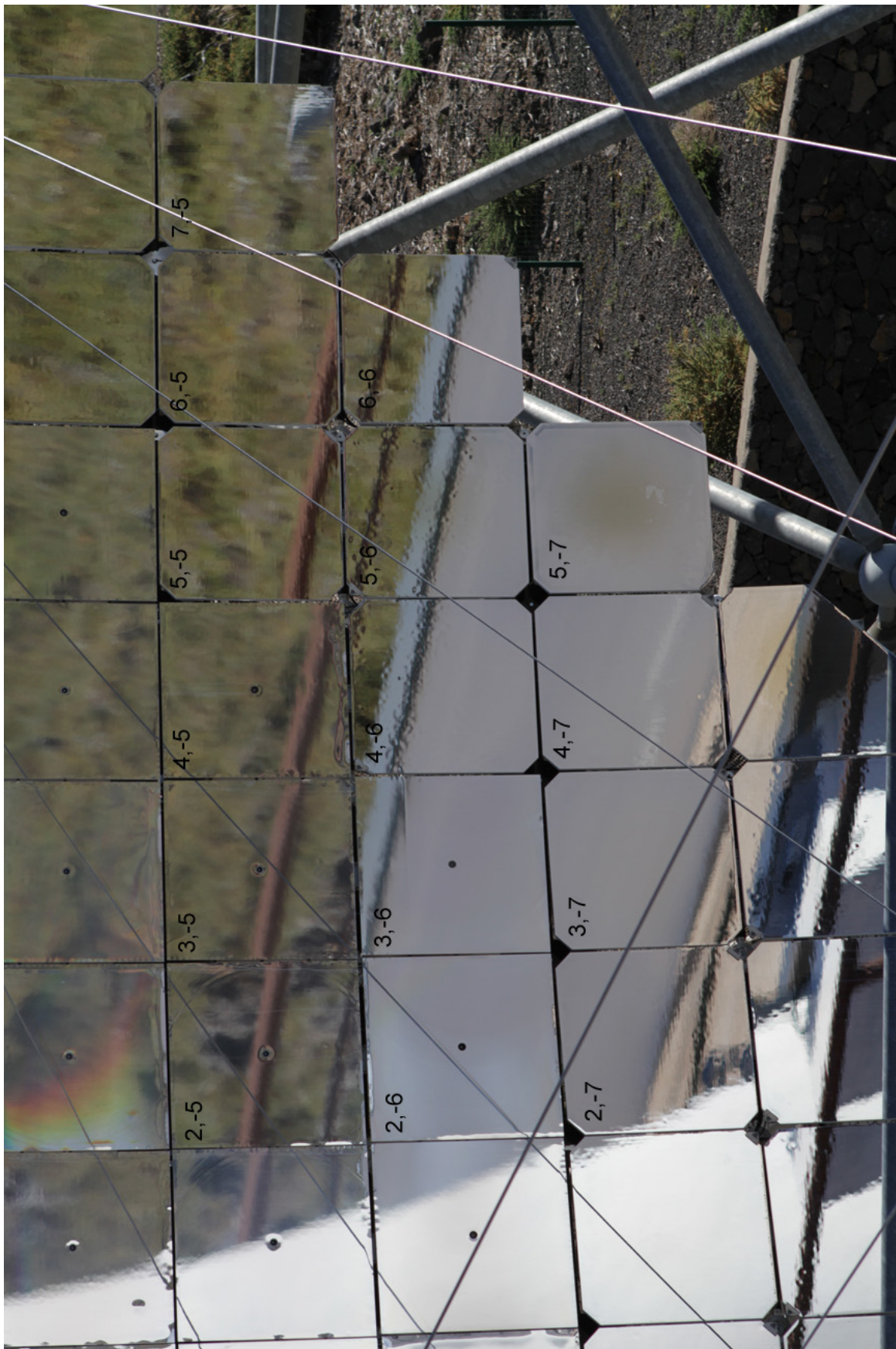












B REFLECTIVITY MEASUREMENTS OF MAGIC-II MIRRORS

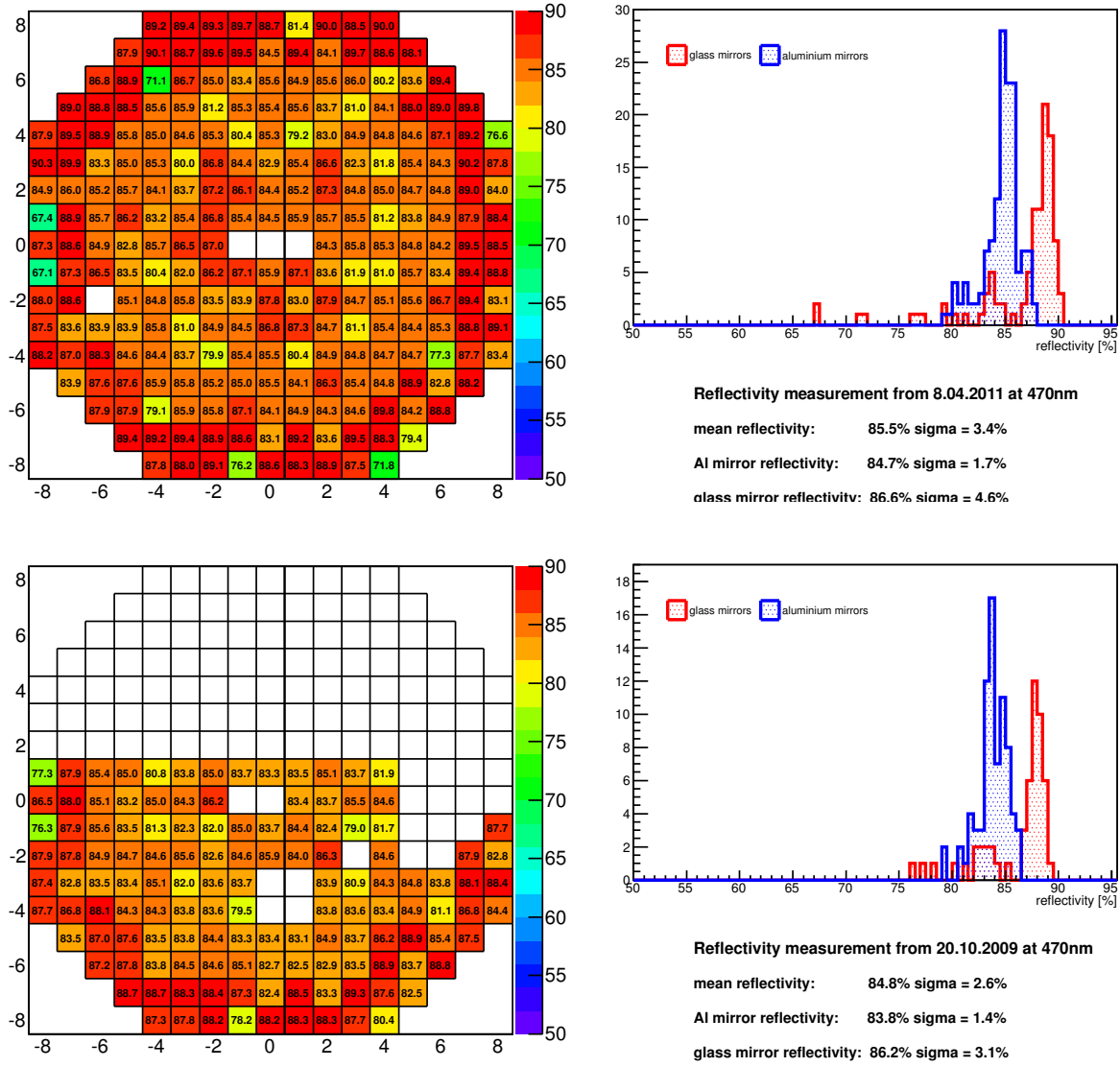


Figure 21: Mirror surface reflectivity at 470 nm.

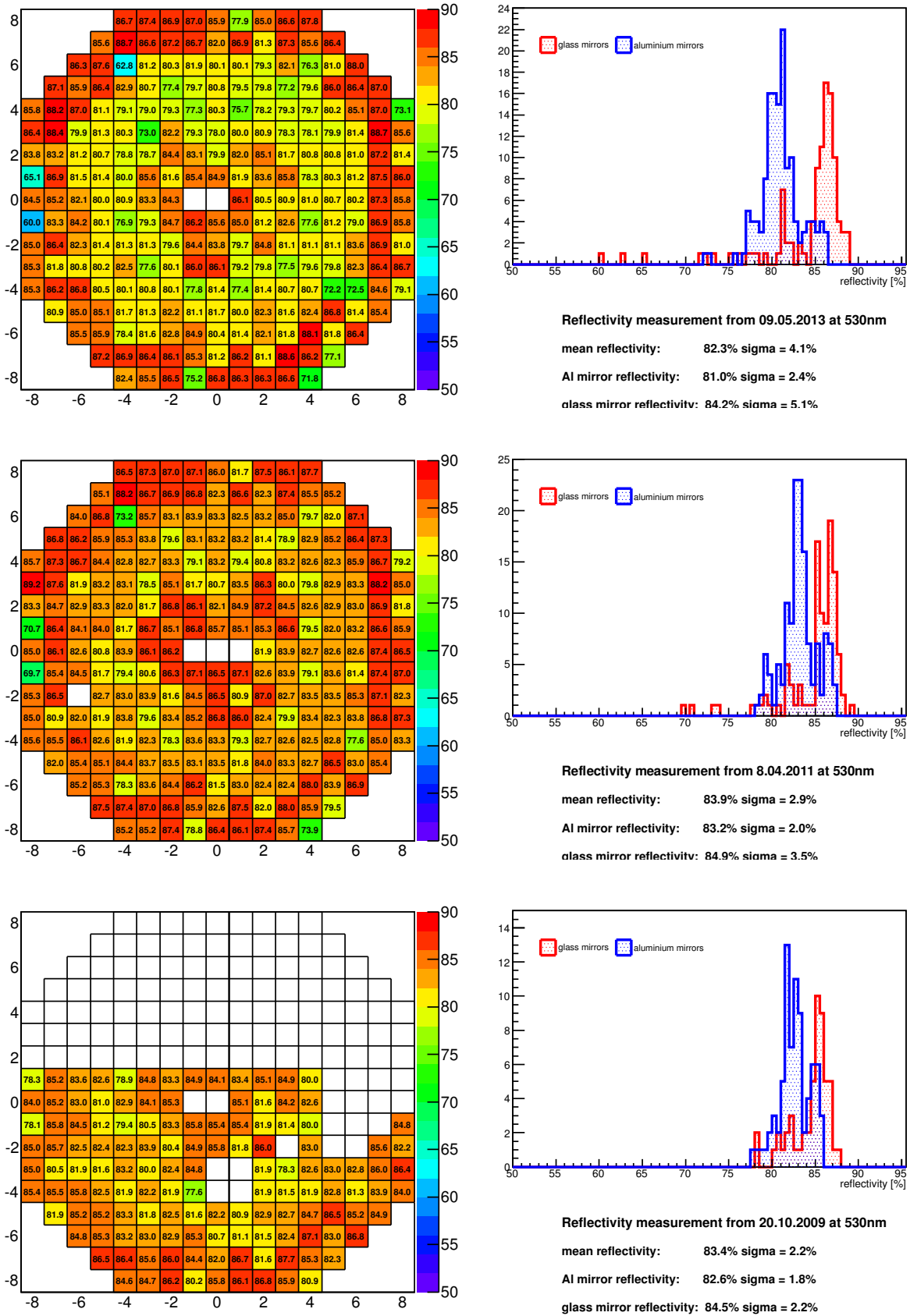


Figure 22: Mirror surface reflectivity at 530 nm.

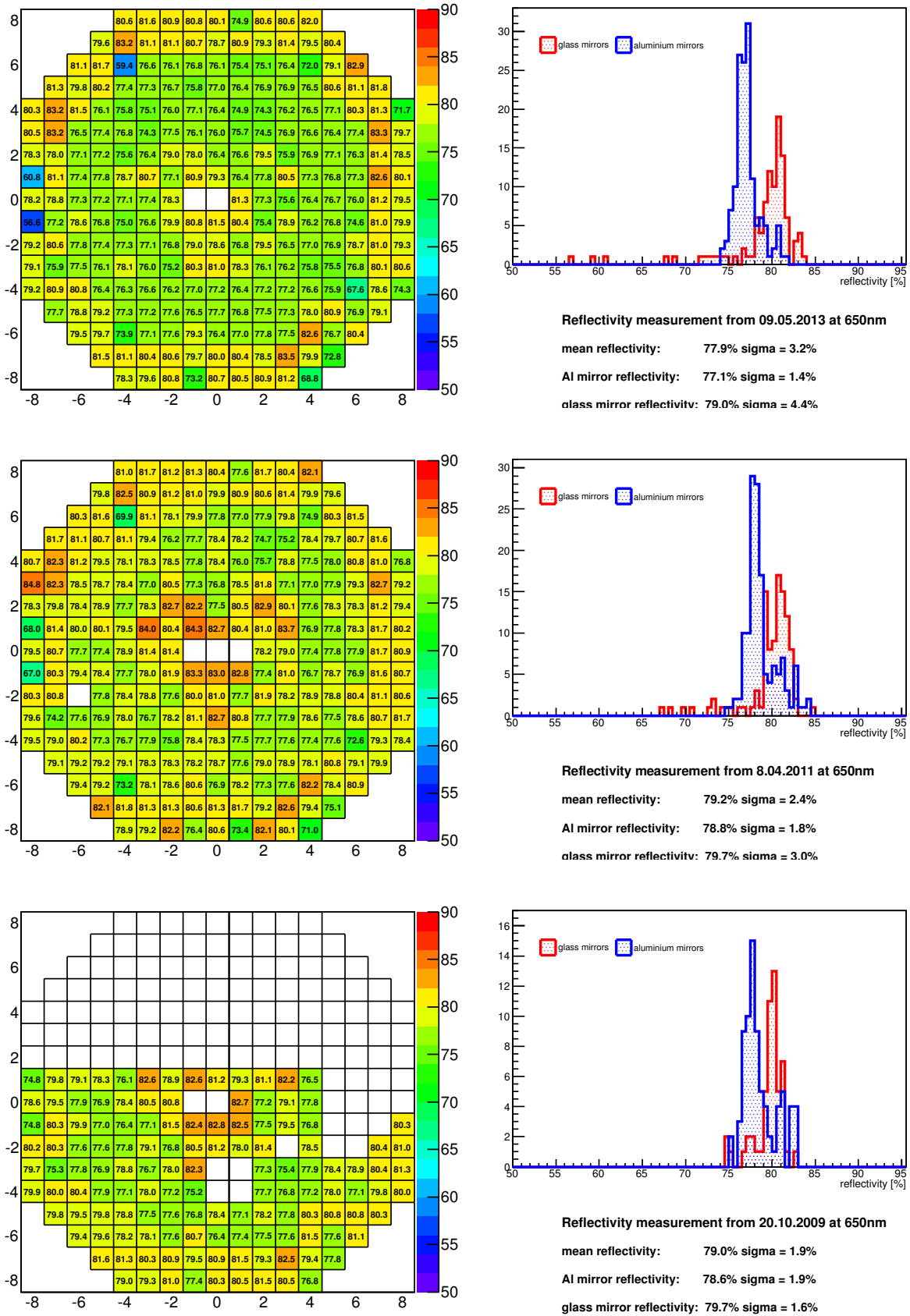


Figure 23: Mirror surface reflectivity at 650 nm.

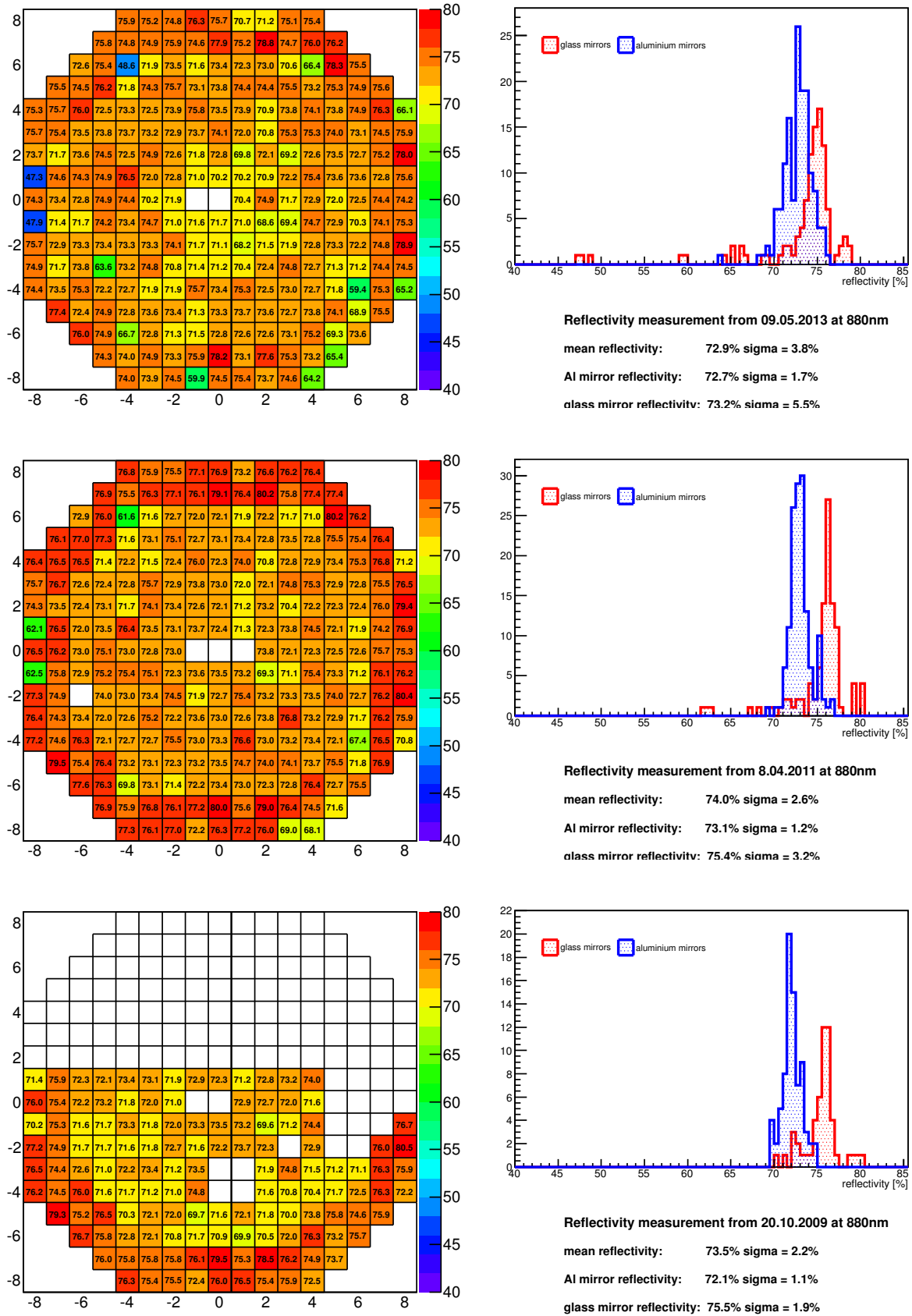


Figure 24: Mirror surface reflectivity at 880 nm.